Mathematical Modelling and Numerical Simulation with Applications, 2024, 4(1), 37–65

https://dergipark.org.tr/en/pub/mmnsa
ISSN Online: 2791-8564 / Open Access
https://doi.org/10.53391/mmnsa.1408997

RESEARCH PAPER

A novel Touchard polynomial-based spectral matrix collocation method for solving the Lotka-Volterra competition system with diffusion

Mohammad Izadi [1,‡], **Ahmed El-Mesady** [2,*,‡] **and Waleed Adel** [3,4,‡]

[1]Department of Applied Mathematics, Faculty of Mathematics and Computer, Shahid Bahonar University of Kerman, Kerman, Iran, [2]Department of Physics and Engineering Mathematics, Faculty of Electronic Engineering, Menoufia University, Menouf, 32952, Egypt, [3]Laboratoire Interdisciplinaire de l'Universite´ Francaise d'Egypte (UFEID Lab), Universite´ Francaise d'Egypte, Cairo, 11837, Egypt, [4]Department of Mathematics and Engineering Physics, Faculty of Engineering, Mansoura University, 35511, Egypt

*Corresponding Author
‡ izadi@uk.ac.ir (Mohammad Izadi); ahmed.ibrahiem81@el-eng.menofia.edu.eg (Ahmed El-Mesady); waleed.ouf@ufe.edu.eg (Waleed Adel)

Abstract

This paper presents the computational solutions of a time-dependent nonlinear system of partial differential equations (PDEs) known as the Lotka-Volterra competition system with diffusion. We propose a combined semi-discretized spectral matrix collocation algorithm to solve this system of PDEs. The first part of the algorithm deals with the time-marching procedure, which is performed using the well-known Taylor series formula. The resulting linear systems of ordinary differential equations (ODEs) are then solved using the spectral matrix collocation technique based on the novel Touchard family of polynomials. We discuss and establish the error analysis and convergence of the proposed method. Additionally, we examine the stability analysis and the equilibrium points of the model to determine the stability condition for the system. We perform numerical simulations using diverse model parameters and with different Dirichlet and Neumann boundary conditions to demonstrate the utility and applicability of our combined Taylor-Touchard spectral collocation algorithm.

Keywords: Collocation points; convergent analysis; stability; Touchard polynomials; Taylor series

AMS 2020 Classification: 65L60; 41A10; 34A12; 35N70; 65L20

1 Introduction

During the past few years, the Lotka-Volterra population model has garnered significant attention from scientists due to its efficacy in describing the interaction between two species in a closed

➤ **Received:** 23.12.2023 ➤ **Revised:** 23.02.2024 ➤ **Accepted:** 09.03.2024 ➤ **Published:** 31.03.2024

ecosystem. Originating in 1925 from the work of renowned scientist Alfred Lotka and independently developed by Vito Volterra in 1926, this model has become a cornerstone in ecological, biological, epidemiological, and economic studies [1–4]. One notable application of this model in economics is in modeling the interaction between firms within a market [5], while in epidemiology, it finds use in understanding the spread of infectious diseases [6]. The fundamental assumptions of the model posit that the population sizes of the predator and prey species are determined solely by their interactions with each other and their environment.

Specifically, the model assumes (1) exponential growth of the prey population in the absence of predators, (2) exponential decline of the predator population in the absence of prey, (3) proportional growth of the predator population relative to the prey population, and (4) proportional decline of the prey population relative to the predator population. The simplest form of the Lotka-Volterra population model can be expressed as a system of two coupled first-order ordinary differential equations, one for the prey population and one for the predator population. This formulation serves as a foundational framework for further analysis and applications

$$\begin{cases} \dfrac{dv}{dt} = a\,v - b\,vw, \\ \dfrac{dw}{dt} = -c\,w + d\,vw, \end{cases} \tag{1}$$

where v and w represent the population sizes of the prey and predator, respectively, and a, b, c, and d are parameters governing the growth rates and interactions between the two populations. The Lotka-Volterra model exhibits several intriguing and significant features. Among these is the presence of periodic solutions, which depict the cyclic behavior of predator and prey populations within a closed ecosystem. These cycles, often referred to as predator-prey cycles or limit cycles, are a characteristic aspect of the model.

Moreover, the model has been extended in various ways to encompass more complex ecological interactions. One notable extension is the diffusive Lotka-Volterra competition model, which describes the interactions among two or more competing species within a spatially heterogeneous environment. Unlike the classical Lotka-Volterra competition model, which assumes that the population sizes of competing species are solely determined by their interactions and environment, the diffusive Lotka-Volterra competition system accounts for the effects of spatial heterogeneity on species competition. Given these important variations of the Lotka-Volterra model, numerous efforts have been made to find accurate solutions to such models. For instance, Ni et al. [7] investigated the model's global stability and pattern formation, considering dynamical resources. Lin et al. [8] discussed traveling wave solutions for the delayed Lotka-Volterra model using Schauder's fixed point theorem. Wijeratne et al. [9] conducted a detailed bifurcation analysis for the diffusive model, with potential applications in market share at duopoly, including a case study in Sri Lanka. Cherniha et al. [10] provided a review of up-to-date solutions for the diffusive model, presenting a wide range of exact solutions for its applications.

Numerous other works on the simulation and discussion of dynamics in the diffusive model can be found in [11–14] and references therein. In this research paper, our primary focus is on the approximate solutions of a system of partial differential equations (PDEs) comprising two nonlinear equations with quadratic terms (see [15]):

$$\begin{cases} \frac{\partial v}{\partial \tau} - D_1 \frac{\partial^2 v}{\partial x^2} = v(A_1 - B_1\, v - C_1\, w), \\ \frac{\partial w}{\partial \tau} - D_2 \frac{\partial^2 w}{\partial x^2} = w(A_2 - B_2\, w - C_2\, v), \end{cases} \quad (x,\tau) \in \Omega_L \times \Omega_T, \tag{2}$$

where $\Omega_L := [0, L]$ and $\Omega_T := [0, T]$ with the initial conditions

$$v(x, \tau = 0) = f(x), \quad w(x, \tau = 0) = g(x), \quad x \in \Omega_L. \tag{3}$$

Here, by $v = v(x,\tau)$ and $w = w(x,\tau)$ we denote the population densities of two given competing species at time τ and f, g are two (smooth) given functions. Also, D_1 and D_2 are diffusion coefficients and are assumed to be positive constants. The non-negative constants A_1, A_2 show the growth rate of the respective species, $B_1, B_2 \geq 0$ represent the related dead rates, and $C_1, C_2 \geq 0$ are the interaction rates between two competing species. The boundary conditions are supplemented either in the form of Dirichlet

$$\begin{cases} v(x = 0, \tau) = v_0(\tau), & v(x = L, \tau) = v_L(\tau), \\ w(x = 0, \tau) = w_0(\tau), & w(x = L, \tau) = w_L(\tau), \end{cases} \quad \tau \in \Omega_T, \tag{4}$$

or as the Neumann boundary conditions are given by

$$\begin{cases} \frac{\partial v}{\partial x}(x = 0, \tau) = v_0(\tau), & \frac{\partial v}{\partial x}(x = L, \tau) = v_L(\tau), \\ \frac{\partial w}{\partial x}(x = 0, \tau) = w_0(\tau), & \frac{\partial w}{\partial x}(x = L, \tau) = w_L(\tau), \end{cases} \quad \tau \in \Omega_T, \tag{5}$$

where the functions $v_0(\tau), w_0(\tau), v_L(\tau)$, and $w_L(\tau)$ are some familiar functions. A few analytical and computational strategies have been developed to deal with the model problem (2) with initial condition (3) accompanied with boundary condition (4) or (5). Let us mention the G'/G-expansion approach [16], the finite difference scheme [17], and the compact implicit-explicit RK type techniques [18]. To acquire the approximate solution of model (2) along with its conditions, we shall adopt a spectral matrix collocation algorithm based on a novel Touchard family of polynomials accompanied by the Taylor expansion technique [19–22]. The applications of the spectral collocation approach with exponential-order accuracy have been examined for various model problems in physical sciences. For example, we may draw your attention to the recently published works [23–30]. The Touchard polynomials, also known as Touchard-Riordan polynomials or exponential polynomials, constitute a family of functions prominent in combinatorics and partition theory [31]. Named after the French mathematician Jacques Touchard, who introduced them in 1934, these polynomials are defined through exponential generating functions and exhibit close ties to Bell polynomials and Stirling numbers of the second kind [32].

Offering several intriguing properties, they find applications across various mathematical domains, including combinatorics, number theory, and algebraic geometry. Their utility extends to the realm of modeling, where they have been increasingly employed in recent years. Touchard polynomials have found utility in analyzing stochastic models such as branching processes, random walks, and queueing systems. In these contexts, they have been instrumental in deriving exact and asymptotic expressions for key parameters, including the probability of extinction, expected particle counts,

and waiting time distributions. Despite their versatility, their application in solving mathematical models has been relatively limited. For instance, Sabermahani [33] adapted Touchard polynomials to solve fractional-order Fokker-Planck equations, representing one of the few reported instances of their use in mathematical modeling. Motivated by this gap in the literature, the current study explores the application of Touchard polynomials in simulating the model described in (2). As far as the authors are aware, this represents the first instance of Touchard polynomials being utilized to solve diffusive Lotka-Volterra competition systems.
The manuscript is structured as follows: Section 2 introduces the time-advancement approach used for discretizing the time variable in the main model. In Section 3, we conduct a stability analysis of the model, identifying equilibrium points and discussing the conditions for stable solutions. Section 4 provides a comprehensive review of Touchard polynomials, highlighting their relevant properties for subsequent sections. The hybrid Taylor-Touchard algorithm is then elaborated upon in Section 5, followed by a validation of the theoretical framework through several examples in Section 6. Finally, Section 7 presents the conclusions drawn from the study.

2 Time-advancement approach

Here and in this part, we first apply the Taylor formula to discretize the given system of PDEs (2) in time direction. For this purpose, we consider a uniform partitioning of $[0, T]$ into K subdivisions with nodes

$$\tau_0 = 0 < \tau_1 = \Delta\tau < \ldots < \tau_K = K\Delta\tau = T.$$

Here $\Delta\tau = \tau_{k+1} - \tau_k$ indicates the time step of the mesh for $k \in \mathbb{K} := \{0, 1, \ldots, K-1\}$. By v^k, w^k, we denote the approximations to the true exact solutions $v(x,\tau), w(x,\tau)$ at time level τ_k, respectively. Namely, we set

$$v^k \equiv v^k(x) := v(x,\tau_k), \quad w^k \equiv w^k(x) := w(x,\tau_k), \quad x \in \Omega_L.$$

The given equations at time step τ_k are

$$\begin{cases} v^k_\tau = D_1\, v^k_{xx} + A_1\, v^k - B_1\, (v^k)^2 - C_1\, v^k\, w^k, \\ w^k_\tau = D_2\, w^k_{xx} + A_2\, w^k - B_2\, (w^k)^2 - C_2\, v^k\, w^k. \end{cases} \tag{6}$$

Using the Taylor series formula, we find that

$$\begin{cases} v^k_\tau = (v^{k+1} - v^k)/\Delta\tau + \Delta\tau\, v^k_{\tau\tau}/2 + \mathcal{O}(\Delta\tau^2), \\ w^k_\tau = (w^{k+1} - w^k)/\Delta\tau + \Delta\tau\, w^k_{\tau\tau}/2 + \mathcal{O}(\Delta\tau^2), \end{cases} \tag{7}$$

if we differentiate system (6) with regard to τ, we shall have

$$\begin{cases} \Delta\tau\, v^k_{\tau\tau} & = D_1(v^{k+1}_{xx} - v^k_{xx}) + A_1(v^{k+1} - v^k) - 2B_1\, v^k(v^{k+1} - v^k) - C_1\, (v^{k+1} - v^k)\, w^k \\ & \quad -C_1\, v^k(w^{k+1} - w^k), \\ \Delta\tau\, w^k_{\tau\tau} & = D_2(w^{k+1}_{xx} - w^k_{xx}) + A_2(w^{k+1} - w^k) - 2B_2\, w^k(w^{k+1} - w^k) - C_2\, v^k\, (w^{k+1} - w^k) \\ & \quad -C_2(v^{k+1} - v^k)w^k, \end{cases} \tag{8}$$

in which we have replaced all terms in the forms v_τ^k, w_τ^k by their difference first-order quotients $(v^{k+1}-v^k)/\Delta\tau$, $(w^{k+1}-w^k)/\Delta\tau$ respectively on the right-hand side.

Now, it is sufficient to insert the two above relations (8) into (7). Then, the left-hand sides of relations (7) will be equated to those related relations given in (6). After some manipulations and collecting the same terms together, we reach the discretized linearized set of equations for (2). In the matrix form, we get

$$\boldsymbol{M}_1^k(x)\frac{d^2}{dx^2}\boldsymbol{U}^{k+1}(x)+\boldsymbol{M}_2^k(x)\,\boldsymbol{U}^{k+1}(x)=\boldsymbol{H}^k(x),\quad k\in\mathbb{K}, \tag{9}$$

where

$$\boldsymbol{U}^{k+1}(x):=\begin{bmatrix}v^{k+1}\\ w^{k+1}\end{bmatrix},\ \boldsymbol{M}_1^k(x):=\begin{bmatrix}-D_1\,\Delta\tau & 0\\ 0 & -D_2\,\Delta\tau\end{bmatrix},\ \boldsymbol{H}^k(x):=\begin{bmatrix}D_1\,\Delta\tau\,v_{xx}^k+(2+A_1\,\Delta\tau)v^k\\ D_2\,\Delta\tau\,w_{xx}^k+(2+A_2\,\Delta\tau)w^k\end{bmatrix},$$

and

$$\boldsymbol{M}_2^k(x):=\begin{bmatrix}2+\Delta\tau\left(-A_1+2B_1\,v^k+C_1\,w^k\right) & C_1\,\Delta\tau\,v^k\\ C_2\,\Delta\tau\,w^k & 2+\Delta\tau\left(-A_2+2B_2\,w^k+C_2\,v^k\right)\end{bmatrix}.$$

To compute the approximate solution of Eq. (9), one first requires the expression $\boldsymbol{U}^0(x)$, which is obtained from the initial conditions $v^0(x)=f(x)$ and $w^0(x)=g(x)$. Besides the functions $v^0(x)=f(x)$ and $w^0(x)=g(x)$, the second-order derivative of them also appears in the vector function $\boldsymbol{H}^0(x)$. The boundary conditions (4) or (5) will be converted accordingly. Under the prescription of Dirichlet boundary conditions we have the following at $x=0,L$

$$\boldsymbol{U}^{k+1}(0)=\boldsymbol{B}_0^{k+1}:=\begin{bmatrix}v_0^{k+1}\\ w_0^{k+1}\end{bmatrix}=\begin{bmatrix}v_0(\tau_{k+1})\\ w_0(\tau_{k+1})\end{bmatrix},\quad \boldsymbol{U}^{k+1}(L)=\boldsymbol{B}_L^{k+1}:=\begin{bmatrix}v_L^{k+1}\\ w_L^{k+1}\end{bmatrix}=\begin{bmatrix}v_L(\tau_{k+1})\\ w_L(\tau_{k+1})\end{bmatrix}. \tag{10}$$

In an analog manner, we can handle the Neumann boundary conditions (5) as

$$\frac{d}{dx}\boldsymbol{U}^{k+1}(0)=\boldsymbol{B}_0^{k+1},\qquad \frac{d}{dx}\boldsymbol{U}^{k+1}(L)=\boldsymbol{B}_L^{k+1}, \tag{11}$$

where two vectors $\boldsymbol{B}_0^{k+1}$ and $\boldsymbol{B}_L^{k+1}$ are defined in system (10).

3 Qualitative analysis of the model

This section is devoted to the qualitative study of the Lotka-Voltral PDE model (2). First, we derive the equilibria of system (2). Then, we discuss the stability of each point.

The equilibrium points of the system

Let us consider both non-diffusive model

$$\begin{cases}\dfrac{dv}{dt}=v(A_1-B_1\,v-C_1\,w),\\ \dfrac{dw}{dt}=w(A_2-B_2\,w-C_2\,v),\end{cases} \tag{12}$$

and diffusive model

$$\begin{cases} \dfrac{\partial v}{\partial \tau} - D_1 \dfrac{\partial^2 v}{\partial x^2} = v(A_1 - B_1\, v - C_1\, w), \\ \dfrac{\partial w}{\partial \tau} - D_2 \dfrac{\partial^2 w}{\partial x^2} = w(A_2 - B_2\, w - C_2\, v), \end{cases} \qquad (x, \tau) \in \Omega_L \times \Omega_T. \tag{13}$$

The equilibrium points of these systems are obtained by equating the right-hand side of system (13) to zero as follows [34, 35]:

$$\begin{cases} v(A_1 - B_1\, v - C_1\, w) = 0, \\ \\ w(A_2 - B_2\, w - C_2\, v) = 0. \end{cases} \tag{14}$$

Hence, by solving the system (14), the equilibrium points of this system are as follows:

$$\begin{cases} (v^1, w^1) = (0, 0), \\ (v^2, w^2) = (0, \dfrac{A_2}{B_2}), \\ (v^3, w^3) = (\dfrac{A_1}{B_1}, 0), \\ (v^4, w^4) = (\dfrac{A_1 B_2 - A_2 C_1}{B_1 B_2 - C_1 C_2}, \dfrac{A_2 B_1 - A_1 C_2}{B_1 B_2 - C_1 C_2}). \end{cases} \tag{15}$$

The stability of the equilibrium points

The non-diffusive model can be described by the following system:

$$\begin{cases} \dfrac{dv}{dt} = v(A_1 - B_1\, v - C_1\, w) = \varphi(v, w), \\ \dfrac{dw}{dt} = w(A_2 - B_2\, w - C_2\, v) = \psi(v, w). \end{cases} \tag{16}$$

The Jacobian matrix corresponding to system (16) is as follows:

$$J = \begin{bmatrix} \dfrac{\partial \varphi}{\partial v} & \dfrac{\partial \varphi}{\partial w} \\ \dfrac{\partial \psi}{\partial v} & \dfrac{\partial \psi}{\partial w} \end{bmatrix}.$$

The characteristic equation can be represented by

$$\lambda^2 - \left(\frac{\partial \varphi}{\partial v} + \frac{\partial \psi}{\partial w} \right) \lambda + \left(\frac{\partial \varphi}{\partial v} \frac{\partial \psi}{\partial w} - \frac{\partial \varphi}{\partial w} \frac{\partial \psi}{\partial v} \right) = 0. \tag{17}$$

Suppose that we are at the steady state $v = v^{ss}, w = w^{ss}$. Therefore, we can conclude that the equilibrium point (v^{ss}, w^{ss}) is locally asymptotically stable according to Routh–Hurwitz criteria if

the next conditions are fulfilled at the equilibrium point

$$\begin{cases} \dfrac{\partial \varphi}{\partial v} + \dfrac{\partial \psi}{\partial w} < 0, \\ \dfrac{\partial \varphi}{\partial v}\dfrac{\partial \psi}{\partial w} - \dfrac{\partial \varphi}{\partial w}\dfrac{\partial \psi}{\partial v} > 0. \end{cases} \tag{18}$$

From system (16), we have

$$\begin{cases} \dfrac{\partial \varphi}{\partial v} = A_1 - 2B_1\, v - C_1\, w, \\ \dfrac{\partial \varphi}{\partial w} = -C_1\, v, \\ \dfrac{\partial \psi}{\partial v} = -C_2\, v, \\ \dfrac{\partial \psi}{\partial w} = A_2 - 2B_2\, w - C_2\, v. \end{cases} \tag{19}$$

Since we have four equilibrium points, there are four cases:
Case 1: For $(v^{ss}, w^{ss}) = (v^1, w^1) = (0, 0)$, the partial derivatives in (19) can be written as follows:

$$\begin{cases} \dfrac{\partial \varphi}{\partial v} = A_1, \\ \dfrac{\partial \varphi}{\partial w} = 0, \\ \dfrac{\partial \psi}{\partial v} = 0, \\ \dfrac{\partial \psi}{\partial w} = A_2. \end{cases} \tag{20}$$

Therefore, we can write

$$\begin{cases} \dfrac{\partial \varphi}{\partial v} + \dfrac{\partial \psi}{\partial w} = A_1 + A_2 \geq 0, \\ \dfrac{\partial \varphi}{\partial v}\dfrac{\partial \psi}{\partial w} - \dfrac{\partial \varphi}{\partial w}\dfrac{\partial \psi}{\partial v} = A_1 A_2 \geq 0. \end{cases} \tag{21}$$

Hence the equilibrium point $(v^1, w^1) = (0, 0)$ is unstable.
Case 2: For $(v^{ss}, w^{ss}) = (v^2, w^2) = (0, \frac{A_2}{B_2})$, the partial derivatives in (19) can be written as follows:

$$\begin{cases} \dfrac{\partial \varphi}{\partial v} = A_1 - C_1 \dfrac{A_2}{B_2}, \\ \dfrac{\partial \varphi}{\partial w} = 0, \\ \dfrac{\partial \psi}{\partial v} = 0, \\ \dfrac{\partial \psi}{\partial w} = -A_2. \end{cases} \tag{22}$$

Consequently, we can write

$$\begin{cases} \dfrac{\partial \varphi}{\partial v} + \dfrac{\partial \psi}{\partial w} = A_1 - C_1\dfrac{A_2}{B_2} - A_2, \\ \dfrac{\partial \varphi}{\partial v}\dfrac{\partial \psi}{\partial w} - \dfrac{\partial \varphi}{\partial w}\dfrac{\partial \psi}{\partial v} = (C_1\dfrac{A_2}{B_2} - A_1)A_2. \end{cases} \tag{23}$$

Hence the equilibrium point $(v^2, w^2) = (0, \frac{A_2}{B_2})$ will be asymptotically stable if $A_1 - C_1\frac{A_2}{B_2} - A_2 < 0$ and $(C_1\frac{A_2}{B_2} - A_1)A_2 > 0$.

Case 3: For $(v^{ss}, w^{ss}) = (v^3, w^3) = (\frac{A_1}{B_1}, 0)$, the partial derivatives in (19) can be written as follows:

$$\begin{cases} \dfrac{\partial \varphi}{\partial v} = -A_1, \\ \dfrac{\partial \varphi}{\partial w} = -C_1\dfrac{A_1}{B_1}, \\ \dfrac{\partial \psi}{\partial v} = -C_2\dfrac{A_1}{B_1}, \\ \dfrac{\partial \psi}{\partial w} = A_2 - C_2\dfrac{A_1}{B_1}. \end{cases} \tag{24}$$

Thus, we can write

$$\begin{cases} \dfrac{\partial \varphi}{\partial v} + \dfrac{\partial \psi}{\partial w} = A_2 - A_1 - C_2\dfrac{A_1}{B_1}, \\ \dfrac{\partial \varphi}{\partial v}\dfrac{\partial \psi}{\partial w} - \dfrac{\partial \varphi}{\partial w}\dfrac{\partial \psi}{\partial v} = (C_2\dfrac{A_1}{B_1} - A_2)A_1 - C_1C_2(\dfrac{A_1}{B_1})^2. \end{cases} \tag{25}$$

Hence, the equilibrium point $(v^3, w^3) = (\frac{A_1}{B_1}, 0)$ will be asymptotically stable if $A_2 - A_1 - C_2\frac{A_1}{B_1} < 0$ and $(C_2\frac{A_1}{B_1} - A_2)A_1 - C_1C_2(\frac{A_1}{B_1})^2 > 0$.

Case 4: For $(v^{ss}, w^{ss}) = (v^4, w^4) = (\frac{A_1B_2 - A_2C_1}{B_1B_2 - C_1C_2}, \frac{A_2B_1 - A_1C_2}{B_1B_2 - C_1C_2})$, the partial derivatives in (19) can be written as follows:

$$\begin{cases} \dfrac{\partial \varphi}{\partial v} = A_1 - 2B_1(\dfrac{A_1B_2 - A_2C_1}{B_1B_2 - C_1C_2}) - C_1(\dfrac{A_2B_1 - A_1C_2}{B_1B_2 - C_1C_2}), \\ \dfrac{\partial \varphi}{\partial w} = -C_1(\dfrac{A_1B_2 - A_2C_1}{B_1B_2 - C_1C_2}), \\ \dfrac{\partial \psi}{\partial v} = -C_2(\dfrac{A_1B_2 - A_2C_1}{B_1B_2 - C_1C_2}), \\ \dfrac{\partial \psi}{\partial w} = A_2 - 2B_2(\dfrac{A_2B_1 - A_1C_2}{B_1B_2 - C_1C_2}) - C_2(\dfrac{A_1B_2 - A_2C_1}{B_1B_2 - C_1C_2}). \end{cases} \tag{26}$$

Hence the equilibrium point $(v^4, w^4) = (\frac{A_1B_2-A_2C_1}{B_1B_2-C_1C_2}, \frac{A_2B_1-A_1C_2}{B_1B_2-C_1C_2})$ is asymptotically stable if

$$\begin{aligned}
\frac{\partial \varphi}{\partial v} + \frac{\partial \psi}{\partial w} &= A_1 - 2B_1(\frac{A_1B_2 - A_2C_1}{B_1B_2 - C_1C_2}) - C_1(\frac{A_2B_1 - A_1C_2}{B_1B_2 - C_1C_2}) \\
&\quad + A_2 - 2B_2(\frac{A_2B_1 - A_1C_2}{B_1B_2 - C_1C_2}) - C_2(\frac{A_1B_2 - A_2C_1}{B_1B_2 - C_1C_2)} < 0, \\
\frac{\partial \varphi}{\partial v}\frac{\partial \psi}{\partial w} - \frac{\partial \varphi}{\partial w}\frac{\partial \psi}{\partial v} &= (A_1 - 2B_1(\frac{A_1B_2 - A_2C_1}{B_1B_2 - C_1C_2}) - C_1(\frac{A_2B_1 - A_1C_2}{B_1B_2 - C_1C_2})) \\
&\quad \times (A_2 - 2B_2(\frac{A_2B_1 - A_1C_2}{B_1B_2 - C_1C_2}) - C_2(\frac{A_1B_2 - A_2C_1}{B_1B_2 - C_1C_2})) \\
&\quad - C_1C_2(\frac{A_1B_2 - A_2C_1}{B_1B_2 - C_1C_2})^2 > 0.
\end{aligned} \tag{27}$$

The diffusive model can be written as follows:

$$\begin{cases}
\dfrac{\partial v}{\partial \tau} = D_1 \dfrac{\partial^2 v}{\partial x^2} + \varphi(u, v), \\
\dfrac{\partial w}{\partial \tau} = D_2 \dfrac{\partial^2 w}{\partial x^2} + \psi(u, v).
\end{cases} \tag{28}$$

Now, we linearize the diffusive model by taking $\tilde{v} = v - v_{ss}$ and $\tilde{w} = w - w_{ss}$. Hence, system (28) is transformed to

$$\begin{cases}
\dfrac{\partial \tilde{v}}{\partial \tau} = D_1 \dfrac{\partial^2 \tilde{v}}{\partial x^2} + \dfrac{\partial \varphi}{\partial v}\tilde{v} + \dfrac{\partial \varphi}{\partial w}\tilde{w}, \\
\dfrac{\partial \tilde{w}}{\partial \tau} = D_2 \dfrac{\partial^2 \tilde{w}}{\partial x^2} + \dfrac{\partial \psi}{\partial v}\tilde{v} + \dfrac{\partial \psi}{\partial w}\tilde{w}.
\end{cases} \tag{29}$$

By taking $\tilde{v}(x,t) = v^* e^{\sigma t} \sin \alpha x$ and $\tilde{w}(x,t) = w^* e^{\sigma t} \sin \alpha x$, then (29) is transformed to

$$\begin{cases}
\sigma v^* = -\alpha^2 D_1 v^* + \dfrac{\partial \varphi}{\partial v} v^* + \dfrac{\partial \varphi}{\partial w} w^*, \\
\sigma w^* = -\alpha^2 D_2 w^* + \dfrac{\partial \psi}{\partial v} v^* + \dfrac{\partial \psi}{\partial w} w^*,
\end{cases} \tag{30}$$

or

$$\begin{cases}
\sigma v^* = (\dfrac{\partial \varphi}{\partial v} - \alpha^2 D_1) v^* + \dfrac{\partial \varphi}{\partial w} w^*, \\
\sigma w^* = \dfrac{\partial \psi}{\partial v} v^* + (\dfrac{\partial \psi}{\partial w} - \alpha^2 D_2) w^*,
\end{cases} \tag{31}$$

which can be written as a linear system as follows:

$$AX = \sigma X, \tag{32}$$

$$A = \begin{bmatrix} \frac{\partial \varphi}{\partial v} - \alpha^2 D_1 & \frac{\partial \varphi}{\partial w} \\ \frac{\partial \psi}{\partial v} & \frac{\partial \psi}{\partial w} - \alpha^2 D_2 \end{bmatrix}, \quad X = \begin{bmatrix} v^* \\ w^* \end{bmatrix}. \tag{33}$$

Hence, the characteristic equation $|A - \sigma I| = 0$, can be represented by

$$\sigma^2 - \left((\frac{\partial \varphi}{\partial v} - \alpha^2 D_1) + (\frac{\partial \psi}{\partial w} - \alpha^2 D_2) \right) \sigma + \left(\frac{\partial \varphi}{\partial v} - \alpha^2 D_1 \right) \left(\frac{\partial \psi}{\partial w} - \alpha^2 D_2 \right) - \frac{\partial \varphi}{\partial w} \frac{\partial \psi}{\partial v} = 0. \tag{34}$$

As a result, the asymptotic stability according to Routh–Hurwitz criterion [34, 35] is verified if

$$\left((\frac{\partial \varphi}{\partial v} - \alpha^2 D_1) + (\frac{\partial \psi}{\partial w} - \alpha^2 D_2) \right) < 0, \ (\frac{\partial \varphi}{\partial v} - \alpha^2 D_1)(\frac{\partial \psi}{\partial w} - \alpha^2 D_2) - \frac{\partial \varphi}{\partial w} \frac{\partial \psi}{\partial v} > 0. \tag{35}$$

As we discussed above we have four equilibrium points, then there are four cases:
Case 1: The equilibrium point $(v^1, w^1) = (0, 0)$ is asymptotically stable if

$$\begin{cases} (\frac{\partial \varphi}{\partial v} - \alpha^2 D_1) + (\frac{\partial \psi}{\partial w} - \alpha^2 D_2) = A_1 + A_2 - \alpha^2 (D_1 + D_2) < 0, \\ (\frac{\partial \varphi}{\partial v} - \alpha^2 D_1)(\frac{\partial \psi}{\partial w} - \alpha^2 D_2) - \frac{\partial \varphi}{\partial w} \frac{\partial \psi}{\partial v} = (A_1 - \alpha^2 D_1)(A_2 - \alpha^2 D_2) > 0. \end{cases} \tag{36}$$

Case 2: The equilibrium point $(v^2, w^2) = (0, \frac{A_2}{B_2})$ is asymptotically stable if

$$\begin{cases} (\frac{\partial \varphi}{\partial v} - \alpha^2 D_1) + (\frac{\partial \psi}{\partial w} - \alpha^2 D_2) = A_1 - A_2 - C_1 \frac{A_2}{B_2} - \alpha^2 (D_1 + D_2) < 0, \\ (\frac{\partial \varphi}{\partial v} - \alpha^2 D_1)(\frac{\partial \psi}{\partial w} - \alpha^2 D_2) - \frac{\partial \varphi}{\partial w} \frac{\partial \psi}{\partial v} = (A_1 - C_1 \frac{A_2}{B_2} - \alpha^2 D_1)(-A_2 - \alpha^2 D_2) > 0. \end{cases} \tag{37}$$

Case 3: The equilibrium point $(v^3, w^3) = (\frac{A_1}{B_1}, 0)$ is asymptotically stable if

$$\begin{cases} (\frac{\partial \varphi}{\partial v} - \alpha^2 D_1) + (\frac{\partial \psi}{\partial w} - \alpha^2 D_2) = -A_1 + A_2 - C_2 \frac{A_1}{B_1} - \alpha^2 (D_1 + D_2) < 0, \\ (\frac{\partial \varphi}{\partial v} - \alpha^2 D_1)(\frac{\partial \psi}{\partial w} - \alpha^2 D_2) - \frac{\partial \varphi}{\partial w} \frac{\partial \psi}{\partial v} = (-A_1 - \alpha^2 D_1)(A_2 - C_2 \frac{A_1}{B_1} - \alpha^2 D_2) > 0. \end{cases} \tag{38}$$

Case 4: The equilibrium point $(v^4, w^4) = (\frac{A_1 B_2 - A_2 C_1}{B_1 B_2 - C_1 C_2}, \frac{A_2 B_1 - A_1 C_2}{B_1 B_2 - C_1 C_2})$ is asymptotically stable if

$$\begin{cases} \left(\frac{\partial \varphi}{\partial v} - \alpha^2 D_1 \right) + \left(\frac{\partial \psi}{\partial w} - \alpha^2 D_2 \right) < 0, \\ \left(\frac{\partial \varphi}{\partial v} - \alpha^2 D_1 \right) \left(\frac{\partial \psi}{\partial w} - \alpha^2 D_2 \right) - \frac{\partial \varphi}{\partial w} \frac{\partial \psi}{\partial v} > 0, \end{cases} \tag{39}$$

where

$$\begin{cases} \dfrac{\partial \varphi}{\partial v} = A_1 - 2B_1 \left(\dfrac{A_1B_2 - A_2C_1}{B_1B_2 - C_1C_2} \right) - C_1 \left(\dfrac{A_2B_1 - A_1C_2}{B_1B_2 - C_1C_2} \right), \\ \dfrac{\partial \varphi}{\partial w} = -C_1 \left(\dfrac{A_1B_2 - A_2C_1}{B_1B_2 - C_1C_2} \right), \\ \dfrac{\partial \psi}{\partial v} = -C_2 \left(\dfrac{A_1B_2 - A_2C_1}{B_1B_2 - C_1C_2} \right), \\ \dfrac{\partial \psi}{\partial w} = A_2 - 2B_2 \left(\dfrac{A_2B_1 - A_1C_2}{B_1B_2 - C_1C_2} \right) - C_2 \left(\dfrac{A_1B_2 - A_2C_1}{B_1B_2 - C_1C_2} \right). \end{cases} \tag{40}$$

4 A review of Touchard polynomials: a convergence analysis

The goal is here to first review the main aspects of the Touchrad polynomials (TPs). Also, we mention some main properties of this set of functions. Next, the convergence analysis of TPs is studied.

An overview of Touchard polynomials

Jacques Touchard was the first who study the Touchard polynomials (TPs) associated with various enumeration problems in number theory related to the permutations [36]. These polynomials are also known as the generalization of Bell polynomials or exponential polynomilas [37]. For more applications and detailed descriptions, we refer to [31, 38, 39].

The TPs are defined through the following Rodriguez-like formula:

$$\mathcal{T}_q(x) = \exp(-x) \left(x \frac{d}{dx} \right)^q \{ \exp(x) \}, \quad q \in \mathbb{N}.$$

We next denote the Stirling number (of the second type) by $S_2(q, i)$. It is defined as [40, Chap. 5]

$$S_2(q, i) := \frac{1}{i!} \sum_{j=1}^{i} (-1)^{i-j} \binom{i}{j} j^q, \quad 1 \leq i \leq q,$$

and if $1 \leq q < i$ we have $S_2(q, i) = 0$. We also set $S_2(0, 0) = 1$ and $S_2(0, i) = 0$ for $i \geq 1$. In fact, the Stirling number indicates the number of partitions of a set of size q into i disjoint nonempty subsets. From these numbers, we have the next definition of TPs:

Definition 1 *The Touchard polynomials on* $[0, 1]$ *are given by*

$$\mathcal{T}_q(x) := \sum_{i=0}^{q} S_2(q, i)\, x^i, \quad q \in \mathbb{N}, \tag{41}$$

and $\mathcal{T}_0(x) := 1$.

It is not difficult to obtain the list of $\mathcal{T}_1(x), \ldots, \mathcal{T}_q(x)$ for $q = 5$ given as follow

$$\begin{aligned}
\mathcal{T}_1(x) &= x, \\
\mathcal{T}_2(x) &= x^2 + x, \\
\mathcal{T}_3(x) &= x^3 + 3x^2 + x, \\
\mathcal{T}_4(x) &= x^4 + 6x^3 + 7x^2 + x, \\
\mathcal{T}_5(x) &= x^5 + 10x^4 + 25x^3 + 15x^2 + x.
\end{aligned}$$

One can evidently see that $\mathcal{T}_q(0) = 0$ for all $q \in \mathbb{N}$. We also have $\mathcal{T}_q(1) = B_q$, where B_q represents the Bell numbers for $q \in \mathbb{N}_0 := \mathbb{N} \cup \{0\}$. By using $B_0 = B_1 = 1$, the values of the first Bell numbers are given as $1, 1, 2, 5, 15, 52, 203, 877$, and 4140.
The next result is about the zeros of TPs. These roots with some modifications can be used as the set of collocation nodes in our proposed spectral collocation algorithm, below. A proof of which was proved in [41]:

Theorem 1 *The zeros of $\mathcal{T}_q(x)$ are real, distinct, and non-positive for all $q \in \mathbb{N}$.*

The following results are useful in the subsequent error analysis of TPs. Let $Q \in \mathbb{N}$ be given. To continue, let us denote the vector of $(Q+1)$ TPs by

$$\boldsymbol{T}_Q(x) := \begin{bmatrix} \mathcal{T}_0(x) & \mathcal{T}_1(x) & \ldots & \mathcal{T}_Q(x) \end{bmatrix}. \tag{42}$$

From this representation, we have:

Lemma 1 *The following representation for $\boldsymbol{T}_Q(x)$ holds*

$$\boldsymbol{T}_Q(x) = \boldsymbol{\Sigma}_Q(x)\, \boldsymbol{P}_Q, \tag{43}$$

where the structured upper-triangular matrix $\boldsymbol{P}_Q$ is constant. It is of size $(Q+1) \times (Q+1)$ and defined as

$$\boldsymbol{P}_Q = \begin{bmatrix}
1 & S_2(1,0) & S_2(2,0) & \ldots & S_2(Q-1,0) & S_2(Q,0) \\
0 & 1 & S_2(2,1) & \ldots & S_2(Q-1,1) & S_2(Q,1) \\
0 & 0 & 1 & \ldots & S_2(Q-1,2) & S_2(Q,2) \\
\vdots & \vdots & \ddots & \ddots & \ddots & \vdots \\
0 & 0 & 0 & \ldots & 1 & S_2(Q,Q-1) \\
0 & 0 & 0 & \ldots & 0 & 1
\end{bmatrix},$$

and the vector $\boldsymbol{\Sigma}_Q(x)$ is

$$\boldsymbol{\Sigma}_Q(x) = \begin{bmatrix} 1 & x & x^2 & \ldots & x^Q \end{bmatrix}.$$

Proof By considering (6) and by induction on $Q \in \mathbb{N}$ we can easily deduce the proof.

The non-singularity of the matrix $\boldsymbol{P}_Q$ is obvious as one can see that $\det(\boldsymbol{P}_Q) = 1$.

Error analysis and convergence result of TPs

The goal is to consider the sequence of TPs on $[0,1]$. We will investigate a convergence result associated with the TPs in a detailed manner. In this respect, one is required to consider a suitable space related to $[0,1]$. We set the weight function as $w(x) := 1$ and define

$$L_w^2[0,1] := \{p : [0,1] \to \mathbb{R} \ : \ p \text{ is measurable and } \|p\|_w < \infty\},$$

with the associated norm as $\|p\|_w := \sqrt{\int_0^1 |p(x)|^2 w(x) dx}$.
Let's assume that a function $p(x) \in L_w^2[0,1]$ is given. By writing the function $p(x)$ in a series form in terms of TPs we have

$$p(x) = \sum_{q=0}^{\infty} \phi_q \mathcal{T}_q(x), \quad x \in [0,1]. \tag{44}$$

The final aim would be to find the coefficients $\phi_q, q \geq 0$ as unknowns. The next finite-dimensional subspace $\mathcal{Z}_Q \subseteq L_w^2[0,1]$ will be considered in practical computing as

$$\mathcal{Z}_Q := \text{Span}\langle \mathcal{T}_0(x), \mathcal{T}_1(x), \ldots, \mathcal{T}_Q(x) \rangle.$$

It is evident that $\mathcal{Z}_Q$ is a closed and finite-dimensional (of dimension $Q+1$) and therefore a complete subspace of $L_w^2[0,1]$. This implies that one finds the finest (best) approximation element $p_\star(x) \in \mathcal{Z}_Q$ such that

$$\|p(x) - p_\star(x)\|_w \leq \|p(x) - r(x)\|_w, \quad \forall r \in \mathcal{Z}_Q.$$

As previously mentioned, we use only the first $(Q+1)$ TPs to approximate $p(x)$. It follows that

$$p(x) \approx p_Q(x) := \sum_{q=0}^{Q} \phi_q \mathcal{T}_q(x), \quad x \in [0,1]. \tag{45}$$

The approximate solution $p_Q(x)$ can be stated concisely as follows

$$p_Q(x) = \boldsymbol{T}_Q(x) \boldsymbol{\Phi}_Q, \tag{46}$$

where $\boldsymbol{T}_Q(x)$ is defined in (7) and the unknowns ϕ_q for $q = 0, 1, \ldots, Q$ will be put in a vector form as

$$\boldsymbol{\Phi}_Q := \begin{bmatrix} \phi_0 & \phi_1 & \ldots & \phi_Q \end{bmatrix}^t.$$

To establish our main result related to the convergence of TPs, we state the following Corollary, which is taken from [42] (without proof):

Corollary 1 *Assume that $p(x)$ has a continuous second derivative on $[-1,1]$. Let $P_N(x)$ denote the*

interpolation polynomials (of degree at most N), based on the $N+1$ *points* $x_i = \cos\left(\frac{2i+1}{N+1}\frac{\pi}{2}\right)$, $i = 0, 1, \ldots, N$. *Then* $P_N(x)$ *converges to* $p(x)$ *on* $[-1, 1]$ *as* $N \to \infty$. *Indeed, we have*

$$|p(x) - P_N(x)| = \mathcal{O}(\frac{1}{\sqrt{N}}). \tag{47}$$

Note that we can extend the above result on a general arbitrary domain $[a, b]$ by using the change of variable $2\bar{x} = a + b + (b - a)x$. This transformation also converts the the Chebyshev nodes x_i on $[-1, 1]$ into the associated points $\bar{x}_i$ on $[a, b]$. Here, we have $a = 0$ and $b = 1$. However, the given upper bound in (47) still is valid.
By increasing the number of bases Q, we will show in the next result that the difference between $p(x)$ and the series form $p_Q(x)$ (45) approaching zero. To do so, let us define the error $E_Q(x) := p(x) - p_Q(x)$.

Theorem 2 *Suppose that* $p_Q(x) = \boldsymbol{T}_Q(x)\boldsymbol{\Phi}_Q$ *indicated the best (closest) approximation to* $p(x)$ *out of space* $\mathcal{Z}_Q$ *and let* $p(x) \in L^2_w[0, 1] \cap C^2[0, 1]$. *Then,* $E_Q(x)$ *converges to zero as* $Q \to \infty$. *Indeed, we have*

$$\|E_Q(x)\|_2 = \mathcal{O}(Q^{-\frac{1}{2}}). \tag{48}$$

Proof We first utilize the fact that $p_Q(x)$ shows the finest approximation to $p(x)$ out of $\mathcal{Z}_Q$. Based on the above discussion, one finds that

$$\|p(x) - p_Q(x)\|_w \leq \|p(x) - r(x)\|_w, \quad \forall r \in \mathcal{Z}_Q. \tag{49}$$

The last inequality (49) is still true for a specific selection for $r(x)$ to be $P_Q(x)$ as in Corollary 1 with $N = Q$. Therefore, we conclude

$$\|p(x) - p_Q(x)\|^2_w \leq \|p(x) - P_Q(x)\|^2_w = \int_0^1 |p(x) - P_Q(x)|^2 \, w(x)dx.$$

Now, by virtue of (47) there is a constant C such that

$$\|p(x) - p_Q(x)\|^2_w \leq \left[\frac{C}{\sqrt{Q}}\right]^2 \int_0^1 w(x)dx.$$

We then evaluate the definite integral, which is equal to one. Taking the square root yields the desired conclusion.

Remark 1 *We remark that we can use the larger interval* $[0, L]$, $(L > 1)$ *instead of unit interval* $[0, 1]$. *This can be done just by changing of variable* $x \to x/L$. *In other words, the above results can be easily extended to* $[0, L]$. *In the computational experiments, we may use a larger interval* $[0, L]$ *rather than* $[0, 1]$.

5 The hybrid Taylor-Touchard algorithm

The solution of the Lotka-Volterra competition system (2) can now be obtained through solving the family of discretized equations (9) together with Dirichlet boundary condition (10) or Neumann boundary conditions (11). Now, suppose that we have the approximate solution of (9) at time level $k-1$ for $k \geq 1$. Evidently, at the first time level, namely $\tau = 0$, we have $\boldsymbol{U}^0(x)$ at hand. We assume that at time step k, we can state the numerical solutions of the system (9) as a finite summation of

$(Q+1)$ Touchard basis functions. It follows that

$$\begin{cases} v^k(x) \approx v_{k,Q}(x) = \sum_{q=0}^{Q} \phi_{q,1}^{(k)} \mathcal{T}_q(x), \\ w^k(x) \approx w_{k,Q}(x) = \sum_{q=0}^{Q} \phi_{q,2}^{(k)} \mathcal{T}_q(x). \end{cases} \tag{50}$$

We now seek the coefficients $\phi_{q,r}^{(k)}$ for $r = 1, 2$ and $q = 0, 1, \ldots, Q$. We may state these unknowns in vectorized forms by

$$\boldsymbol{\Phi}_{Q,r}^{(k)} := \begin{bmatrix} \phi_{0,r}^{(k)} & \phi_{1,r}^{(k)} & \ldots & \phi_{Q,r}^{(k)} \end{bmatrix}^t, \quad r = 1, 2.$$

In accordance to the definition $\boldsymbol{T}_Q(x)$ in (42), one able to represent the foregoing equations (50) as

$$\begin{cases} v_{k,Q}(x) = \boldsymbol{T}_Q(x)\, \boldsymbol{\Phi}_{Q,1}^{(k)}, \\ w_{k,Q}(x) = \boldsymbol{T}_Q(x)\, \boldsymbol{\Phi}_{Q,2}^{(k)}. \end{cases} \tag{51}$$

With the help of relation (43) in Lemma 1, we further rewrite these equations as

$$\begin{cases} v_{k,Q}(x) = \boldsymbol{\Sigma}_Q(x)\, \boldsymbol{P}_Q\, \boldsymbol{\Phi}_{Q,1}^{(k)}, \\ w_{k,Q}(x) = \boldsymbol{\Sigma}_Q(x)\, \boldsymbol{P}_Q\, \boldsymbol{\Phi}_{Q,2}^{(k)}. \end{cases} \tag{52}$$

We now put both approximate solutions into one vector. We set $\boldsymbol{U}_Q^{(k)}(x)$ as an approximation to $\boldsymbol{U}^k(x)$ yielding

$$\boldsymbol{U}^k(x) \approx \boldsymbol{U}_Q^{(k)}(x) := \begin{bmatrix} v_{k,Q}(x) \\ w_{k,Q}(x) \end{bmatrix}. \tag{53}$$

By using the foregoing relations (52), the next matrix representations for $\boldsymbol{U}_Q^{(k)}(x)$ is provided. The proof of which is an easy job.

Lemma 2 *The approximated solution $\boldsymbol{U}_Q^{(k)}(x)$ in (53) has the following matrix representation*

$$\boldsymbol{U}_Q^{(k)}(x) = \widehat{\boldsymbol{\Sigma}}_Q(x)\, \widehat{\boldsymbol{P}}_Q\, \widehat{\boldsymbol{\Phi}}_Q^{(k)}, \tag{54}$$

where

$$\widehat{\boldsymbol{\Sigma}}_Q(x) = \begin{bmatrix} \boldsymbol{\Sigma}_Q(x) & \boldsymbol{0} \\ \boldsymbol{0} & \boldsymbol{\Sigma}_Q(x) \end{bmatrix}, \quad \widehat{\boldsymbol{P}}_Q = \begin{bmatrix} \boldsymbol{P}_Q & \boldsymbol{0} \\ \boldsymbol{0} & \boldsymbol{P}_Q \end{bmatrix}, \quad \widehat{\boldsymbol{\Phi}}_Q^{(k)} = \begin{bmatrix} \boldsymbol{\Phi}_{Q,1}^{(k)} \\ \boldsymbol{\Phi}_{Q,2}^{(k)} \end{bmatrix}.$$

By looking at (51), we find that one needs to approximate $\frac{d^2}{dx^2}\boldsymbol{U}^k(x)$. Thus, we consider the vector form

$$\frac{d^2}{dx^2}\boldsymbol{U}^k(x) \approx \frac{d^2}{dx^2}\boldsymbol{U}_Q^{(k)}(x) := \begin{bmatrix} v_{k,Q}''(x) \\ w_{k,Q}''(x) \end{bmatrix}. \tag{55}$$

To calculate the second-order derivatives of $\boldsymbol{U}_Q^{(k)}(x)$, we return to the relations (53). We have to compute only derivatives of the vector $\boldsymbol{\Sigma}_Q(x)$. A simple calculation yields

$$\frac{d}{dx}\boldsymbol{\Sigma}_Q(x) = \boldsymbol{\Sigma}_Q(x)\,\boldsymbol{E}_Q, \quad \boldsymbol{E}_Q = \begin{bmatrix} 0 & 1 & 0 & \dots & 0 \\ 0 & 0 & 2 & \dots & 0 \\ \vdots & \vdots & 0 & \vdots & \vdots \\ 0 & 0 & 0 & \ddots & Q \\ 0 & 0 & 0 & \dots & 0 \end{bmatrix}_{(Q+1)\times(Q+1)}. \tag{56}$$

If we repeat the differentiation, we arrive at

$$\frac{d^2}{dx^2}\boldsymbol{\Sigma}_Q(x) = \boldsymbol{\Sigma}_Q(x)\,\boldsymbol{E}_Q^2. \tag{57}$$

By combining the last relations (57) and (53) we finally get

$$\begin{cases} v''_{k,Q}(x) = \boldsymbol{\Sigma}_Q(x)\,\boldsymbol{E}_Q^2\,\boldsymbol{P}_Q\,\boldsymbol{\Phi}_{Q,1}^{(k)}, \\ w''_{k,Q}(x) = \boldsymbol{\Sigma}_Q(x)\,\boldsymbol{E}_Q^2\,\boldsymbol{P}_Q\,\boldsymbol{\Phi}_{Q,2}^{(k)}. \end{cases} \tag{58}$$

Lemma 3 *The approximated solution* $\frac{d^2}{dx^2}\boldsymbol{U}_Q^{(k)}(x)$ *in* (55) *has the following matrix representation*

$$\frac{d^2}{dx^2}\boldsymbol{U}_Q^{(k)}(x) = \widehat{\boldsymbol{\Sigma}}_Q(x)\,\widehat{\boldsymbol{E}}_Q\,\widehat{\boldsymbol{P}}_Q\,\widehat{\boldsymbol{\Phi}}_Q^{(k)}, \tag{59}$$

where $\widehat{\boldsymbol{\Phi}}_Q^{(k)}$, $\widehat{\boldsymbol{\Sigma}}_Q(x)$ *and* $\widehat{\boldsymbol{P}}_Q$ *are defined in* (54) *and*

$$\widehat{\boldsymbol{E}}_Q = \begin{bmatrix} \boldsymbol{E}_Q^2 & \boldsymbol{0} \\ \boldsymbol{0} & \boldsymbol{E}_Q^2 \end{bmatrix}.$$

A sequence of collocation points will be used now. This set of points can be selected as the zeros of Touchard polynomials as mentioned in Section 4. However, we use the equally distributed points on $[0, L]$. Since we have to determine $Q+1$ coefficients in the series expansion forms (50), we consider $x_s = sL/Q$ for $s = 0, 1, \dots, Q$ as the collocation points. We now collocate the matrix Eqs. (51) at the aforementioned points to reach at

$$\boldsymbol{M}_1^{k-1}(x_s)\,\frac{d^2}{dx^2}\boldsymbol{U}_Q^k(x_s) + \boldsymbol{M}_2^{k-1}(x_s)\,\boldsymbol{U}_Q^k(x_s) = \boldsymbol{H}^{k-1}(x_s), \quad s = 0, 1, \dots, Q, \tag{60}$$

for $k = 1, 2, \dots, K$. We next introduce two matrices and vectors related to the coefficients of the model as

$$\boldsymbol{N}_{k-1,j} = \begin{pmatrix} \boldsymbol{M}_j^{k-1}(x_0) & \boldsymbol{0} & \dots & \boldsymbol{0} \\ \boldsymbol{0} & \boldsymbol{M}_j^{k-1}(x_1) & \dots & \boldsymbol{0} \\ \vdots & \vdots & \ddots & \vdots \\ \boldsymbol{0} & \boldsymbol{0} & \dots & \boldsymbol{M}_j^{k-1}(x_Q) \end{pmatrix}, \quad j = 1, 2, \quad \boldsymbol{F}_{k-1} = \begin{pmatrix} \boldsymbol{H}^{k-1}(x_0) \\ \boldsymbol{H}^{k-1}(x_1) \\ \vdots \\ \boldsymbol{H}^{k-1}(x_Q) \end{pmatrix}.$$

The following notations will be also set

$$\boldsymbol{V}_k := \begin{bmatrix} \boldsymbol{U}_Q^k(x_0) \\ \boldsymbol{U}_Q^k(x_1) \\ \vdots \\ \boldsymbol{U}_Q^k(x_Q) \end{bmatrix}, \quad \boldsymbol{V}_k'' := \begin{bmatrix} \frac{d^2}{dx^2}\boldsymbol{U}_Q^k(x_0) \\ \frac{d^2}{dx^2}\boldsymbol{U}_Q^k(x_1) \\ \vdots \\ \frac{d^2}{dx^2}\boldsymbol{U}_Q^k(x_Q) \end{bmatrix}.$$

A reformulation of the set of matrix Eqs. (60) can be done by using the former matrix and vector notations. So, we have

$$\boldsymbol{N}_{k-1,1}\,\boldsymbol{V}_k'' + \boldsymbol{N}_{k-1,2}\,\boldsymbol{V}_k = \boldsymbol{F}_{k-1}, \qquad k = 1, 2, \ldots, K. \tag{61}$$

To proceed, we collocate two relations (54) and (59) at the collocation nodes. Therefore, we get

Lemma 4 *The matrix forms of $\boldsymbol{V}_k$ and $\boldsymbol{V}_k''$ are obtained as*

$$\boldsymbol{V}_k = \widetilde{\widehat{\boldsymbol{\Sigma}}}_Q\,\widehat{\boldsymbol{P}}_Q\,\widehat{\boldsymbol{\Phi}}_Q^{(k)}, \qquad \boldsymbol{V}_k'' = \widetilde{\widehat{\boldsymbol{\Sigma}}}_Q\,\widehat{\boldsymbol{E}}_Q\,\widehat{\boldsymbol{P}}_Q\,\widehat{\boldsymbol{\Phi}}_Q^{(k)}. \tag{62}$$

Here, two matrices $\widehat{\boldsymbol{P}}_Q, \widehat{\boldsymbol{\Phi}}_Q^{(k)}$ are defined in (54) and the block-diagonal matrix $\widehat{\boldsymbol{E}}_Q$ is introduced in (59). Also, we have used

$$\widetilde{\widehat{\boldsymbol{\Sigma}}}_Q = [\widehat{\boldsymbol{\Sigma}}_Q(x_0) \quad \widehat{\boldsymbol{\Sigma}}_Q(x_1) \quad \ldots \quad \widehat{\boldsymbol{\Sigma}}_Q(x_Q)]^t,$$

where the matrix $\widehat{\boldsymbol{\Sigma}}_Q$ is previously defined in (54).

By placing two relations in (62) into (61) one gets the next (linear) fundamental matrix equation (FME)

$$\left\{\boldsymbol{N}_{k-1,1}\,\widetilde{\widehat{\boldsymbol{\Sigma}}}_Q\,\widehat{\boldsymbol{E}}_Q + \boldsymbol{N}_{k-1,2}\,\widetilde{\widehat{\boldsymbol{\Sigma}}}_Q\right\}\,\widehat{\boldsymbol{P}}_Q\,\widehat{\boldsymbol{\Phi}}_Q^{(k)} = \boldsymbol{F}_{k-1}, \quad k = 1, 2, \ldots, K.$$

If we rephrase the last equations, we have for $k = 1, 2, \ldots, K$

$$\boldsymbol{W}_k\,\widehat{\boldsymbol{\Phi}}_Q^{(k)} = \boldsymbol{F}_{k-1}, \quad \text{or} \quad [\boldsymbol{W}_k; \boldsymbol{F}_{k-1}], \quad \boldsymbol{W}_k := \left(\boldsymbol{N}_{k-1,1}\,\widetilde{\widehat{\boldsymbol{\Sigma}}}_Q\,\widehat{\boldsymbol{E}}_Q + \boldsymbol{N}_{k-1,2}\,\widetilde{\widehat{\boldsymbol{\Sigma}}}_Q\right)\,\widehat{\boldsymbol{P}}_Q. \tag{63}$$

Still, we are required to implement the boundary conditions (10) or (11) and incorporate them into the matrix Eq. (63). For the first Dirichlet boundary condition in (10), we consider (54) followed by approaching x to zero. Similarly, for the second one, we tend x to L. In both cases, we have

$$\begin{aligned} \boldsymbol{W}_k^0\,\widehat{\boldsymbol{\Phi}}_Q^{(k)} &= \boldsymbol{B}_0^k, \quad \boldsymbol{W}_k^0 := \widehat{\boldsymbol{\Sigma}}_Q(0)\,\widehat{\boldsymbol{P}}_Q, \\ \boldsymbol{W}_k^L\,\widehat{\boldsymbol{\Phi}}_Q^{(k)} &= \boldsymbol{B}_L^k, \quad \boldsymbol{W}_k^L := \widehat{\boldsymbol{\Sigma}}_Q(L)\,\widehat{\boldsymbol{P}}_Q. \end{aligned}$$

If the Neumann boundary conditions (5) are given, we first combine two relations (54) and (56) to

obtain

$$\begin{cases} v'_{k,Q}(x) = \boldsymbol{\Sigma}_Q(x)\, \boldsymbol{E}_Q\, \boldsymbol{P}_Q\, \boldsymbol{\Phi}^{(k)}_{Q,1}, \\ w'_{k,Q}(x) = \boldsymbol{\Sigma}_Q(x)\, \boldsymbol{E}_Q\, \boldsymbol{P}_Q\, \boldsymbol{\Phi}^{(k)}_{Q,2}. \end{cases}$$

Now, we let x approaches to $0, L$ to reach at

$$\begin{aligned} \boldsymbol{W}^0_k\, \widehat{\boldsymbol{\Phi}}^{(k)}_Q &= \boldsymbol{B}^k_0, \quad \boldsymbol{W}^0_k := \widehat{\boldsymbol{\Sigma}}_Q(0)\, \boldsymbol{E}_Q\, \widehat{\boldsymbol{P}}_Q, \\ \boldsymbol{W}^L_k\, \widehat{\boldsymbol{\Phi}}^{(k)}_Q &= \boldsymbol{B}^k_L, \quad \boldsymbol{W}^L_k := \widehat{\boldsymbol{\Sigma}}_Q(L)\, \boldsymbol{E}_Q\, \widehat{\boldsymbol{P}}_Q. \end{aligned}$$

In either case of boundary conditions, we use $[\boldsymbol{W}^0_k, \boldsymbol{B}^k_0]$ or $[\boldsymbol{W}^L_k, \boldsymbol{B}^k_L]$ to substitute the first four rows of the FME $[\boldsymbol{W}_k; \boldsymbol{F}_{k-1}]$. We denote the resultant modified system given by

$$[\widetilde{\boldsymbol{W}}_k; \widetilde{\boldsymbol{F}}_{k-1}], \quad k = 1, 2, \ldots, K. \tag{64}$$

Once we solve (64), the unknown Touchard coefficients $\phi^{(k)}_{q,r}$ for $q = 0, 1, \ldots, Q$ and $r = 1, 2$ are obtained at each time level k for $k = 1, 2, \ldots, K$.
The strategy of the residual error function (REF) will now be utilized to measure the accuracy of the presented Taylor-Touchard collocation procedure. Toward this end, we insert the acquired approximate solutions into (2). Thus, the REFs are defined by the following relations

$$\begin{bmatrix} \mathrm{Res}^{(k)}_{v,Q}(x) \\ \mathrm{Res}^{(k)}_{w,Q}(x) \end{bmatrix} = \left| \boldsymbol{M}^{k-1}_1(x) \frac{d^2}{dx^2} \boldsymbol{U}^k_Q(x) + \boldsymbol{M}^{k-1}_2(x)\, \boldsymbol{U}^k_Q(x) - \boldsymbol{H}^{k-1}(x) \right| \cong 0, \tag{65}$$

for $k = 1, 2, \ldots, K$. We note that the foregoing REF formula is useful especially when the exact solutions of system (2) are out of reach for various values of model parameters.

6 Graphical and numerical results

In this part, diverse simulation experiments are conducted to illustrate the utility of the Taylor-Touchard matrix collocation strategy once applied to the Lotka-Volterra competition model (2). Two test case studies with diverse model parameters are solved numerically to testify to the accuracy and performance of the combined approximation technique. All simulation results are performed by utilizing Matlab version R2021a on a digital computer.

Example 1 *We consider the Lotka-Volterra competition system* (2) *with the next initial conditions [17]*

$$f(x) = g(x) = 0.1 \exp(-8x^2).$$

The Dirichlet boundary conditions are taken as

$$v_0(\tau) = w_0(\tau) = f(0), \quad v_L(\tau) = w_L(\tau) = f(L).$$

In the following diverse coefficient parameters A_i, B_i, C_i, and D_i, for $i = 1, 2$ will be considered.

We first set $Q = 5$. We also use $L, T = 1$ and $\Delta\tau = 0.01$. All parameters are set as unity except that $D_1 = 0.5$. The approximate solutions using the presented Taylor-Touchard method at the first

time level $\tau = \Delta\tau$ are given by

$$v_{1,5}(x) = 0.45827\,x^5 - 1.64989\,x^4 + 2.10134\,x^3 - 0.991429\,x^2 - 0.0182481\,x + 0.1,$$
$$w_{1,5}(x) = 0.377296\,x^5 - 1.39838\,x^4 + 1.83421\,x^3 - 0.889391\,x^2 - 0.0237062\,x + 0.1.$$

The obtained approximations at the last time level $\tau = T$ are as follows

$$v_{100,5}(x) = 0.00744598\,x^5 - 0.012201\,x^4 + 0.0307353\,x^3 - 0.0894343\,x^2 - 0.0365125\,x + 0.1,$$
$$w_{100,5}(x) = 0.00808672\,x^5 - 0.0193222\,x^4 + 0.0294968\,x^3 - 0.049399\,x^2 - 0.0688288\,x + 0.1.$$

Figure 1 shows the whole approximate solutions using the above-mentioned parameters on space-time domain $[0,1] \times [0,1]$. While the left picture presents the population density v, the right plot graphically shows the population density w. The snapshots of the associated REFs defined via (65) are also depicted in Figure 2 at different time levels $\tau = \tau_k$ for $k = 1, 2, \ldots, 100$. It is seen that the same results for both approximate solutions v, w are obtained on the unit square $[0,1] \times [0,1]$. To see the discrepancy, we need to go beyond this domain.

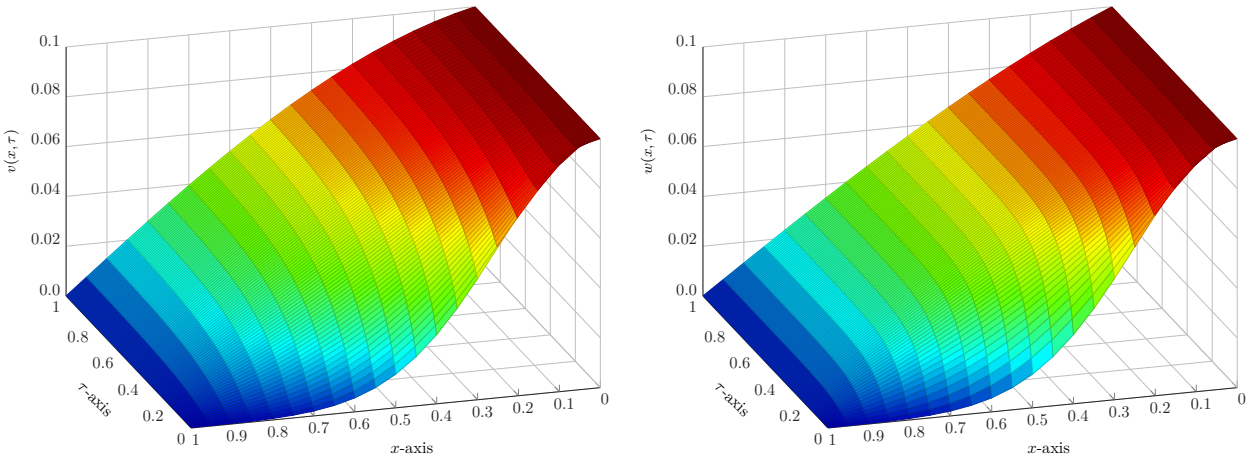

Figure 1. Visualization of approximate solutions $v(x,\tau)$ (left) and $w(x,\tau)$ (right) via Taylor-Touchard matrix algorithm in Example 1 with $Q = 5$, $A_1, A_2 = 1, B_1, B_2 = 1, C_1, C_2 = 1, D_1 = 0.5, D_2 = 1$, $\Delta\tau = 0.01$, for $(x,\tau) \in [0,1] \times [0,1]$.

Let us consider $L = 10$ and $T = 100$ in the computations. In Figure 3, we show the approximate solutions for the population densities v and w using the same parameters as above except that we take a relatively large time step $\Delta\tau = 1$. In fact, the obtained solutions at $\tau = 50$ are given as

$$v_{50,5}(x) = 0.000472878\,x^5 - 0.0149354\,x^4 + 0.168979\,x^3 - 0.836871\,x^2 + 1.66751\,x + 0.1,$$
$$w_{50,5}(x) = 0.0000459759\,x^5 - 0.00140024\,x^4 + 0.0151665\,x^3 - 0.0746089\,x^2 + 0.159923\,x + 0.1.$$

The profile of population densities at $x = 5$ is visualized in Figure 4. One can easily see from Figure 3 and Figure 4 that the population density $v(x,\tau)$ will ultimately survive with low diffusion rates $D_1 = 0.5$ while the second one, $w(x,\tau)$, with higher diffusion value $D_2 = 1$ will die out on $\tau \in [0, 100]$.

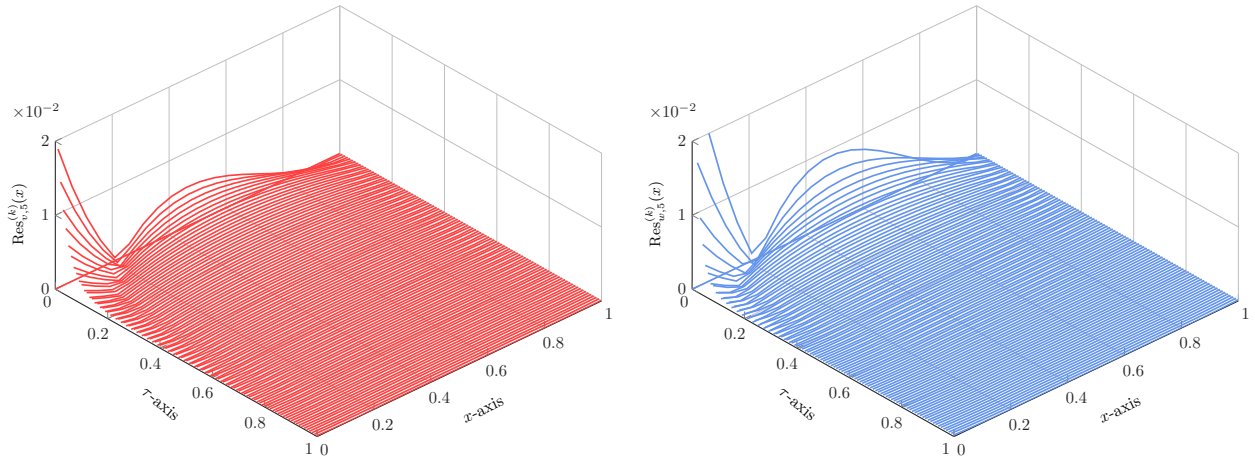

Figure 2. Visualization of REfs $\mathrm{Res}_{v,5}^{(k)}(x)$ (left) and $\mathrm{Res}_{w,5}^{(k)}(x)$ (right) via Taylor-Touchard matrix algorithm in Example 1 with $Q = 5$, $A_1, A_2 = 1, B_1, B_2 = 1, C_1, C_2 = 1, D_1 = 0.5, D_2 = 1$, $\Delta\tau = 0.01$, for $(x, \tau) \in [0, 1] \times [0, 1]$.

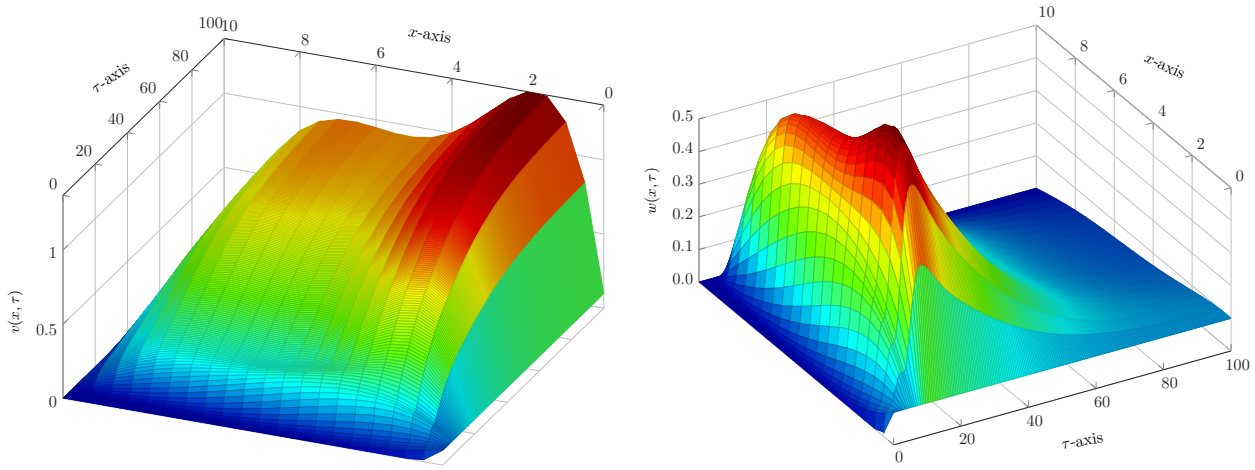

Figure 3. Visualization of approximate solutions $v(x, \tau)$ (left) and $w(x, \tau)$ (right) via Taylor-Touchard matrix algorithm in Example 1 with $Q = 5$, $A_1, A_2 = 1, B_1, B_2 = 1, C_1, C_2 = 1, D_1 = 0.5, D_2 = 1$, $\Delta\tau = 1$, for $(x, \tau) \in [0, 10] \times [0, 100]$.

We next examine the impact of utilizing the growth factors A_1 and A_2 on the interaction between two species. In this respect, we set [17]

$$A_1 = 0.8, \quad A_2 = 1, \quad B_1, B_2 = 1, \quad C_1, C_2 = 1, \quad D_1, D_2 = 1.$$

From these parameters, the following approximations for the competition system are obtained. The two first ones are related to $\tau = \Delta\tau$ as follows

$$v_{1,5}(x) = -2.9310{-}6\,x^5 + 0.000120498\,x^4 - 0.00195727\,x^3 + 0.0157298\,x^2 - 0.0627584\,x + 0.1,$$
$$w_{1,5}(x) = -2.7123{-}6\,x^5 + 0.000112368\,x^4 - 0.00184439\,x^3 + 0.0150341\,x^2 - 0.0611469\,x + 0.1.$$

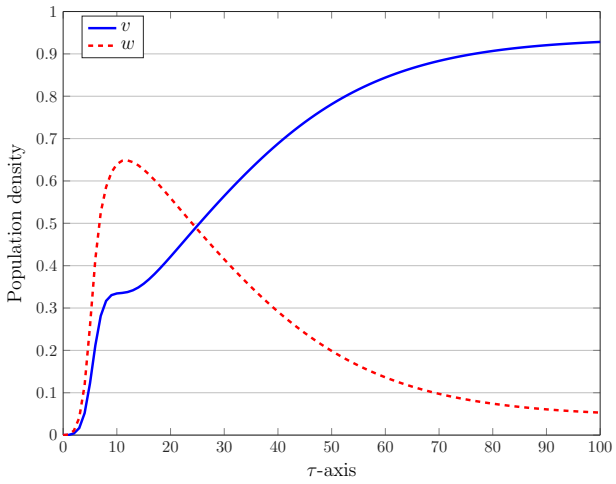

Figure 4. Graphing of population densities via Taylor-Touchard matrix algorithm in Example 1 with $Q = 5$, $A_1, A_2 = 1, B_1, B_2 = 1, C_1, C_2 = 1, D_1 = 0.5, D_2 = 1, \Delta\tau = 1$, at $x = 5$.

The obtained approximations at the final time $\tau = T$ are given by

$$\begin{aligned} v_{100,5}(x) &= -3.31577{-}7\,x^5 + 0.0000265815\,x^4 - 0.000681488\,x^3 + 0.00781148\,x^2 \\ &\quad - 0.0432318\,x + 0.1, \\ w_{100,5}(x) &= 0.000392573\,x^5 - 0.0123676\,x^4 + 0.140267\,x^3 - 0.713172\,x^2 + 1.5369\,x + 0.1. \end{aligned}$$

The graphical representations of two population species are visualized on Figure 5 on the whole domain $(x, \tau) \in [0, 10] \times [0, 100]$. The profile of population densities at $x = 5$ and for $\tau \in [0, 100]$ are depicted on Figure 6.

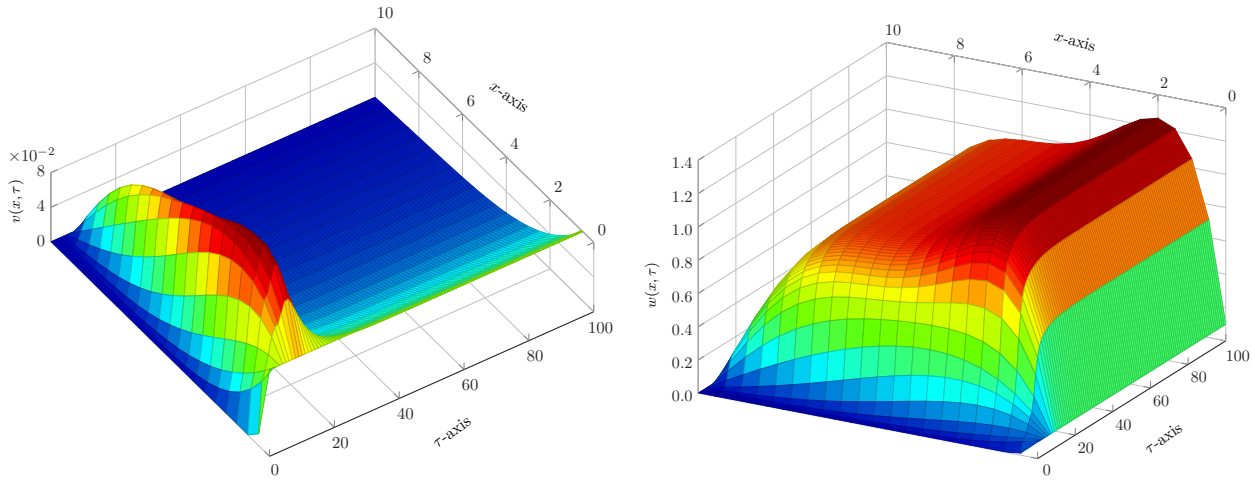

Figure 5. Graphing of approximate solutions $v(x, \tau)$ (left) and $w(x, \tau)$ (right) via Taylor-Touchard matrix algorithm in Example 1 with $Q = 5$, $A_1 = 0.8, A_2 = 1, B_1, B_2 = 1, C_1, C_2 = 1, D_1, D_2 = 1$, $\Delta\tau = 1$, for $(x, \tau) \in [0, 10] \times [0, 100]$.

By looking at the plotted Figure 5 and Figure 6 we infer that under the assumption on the growth rates $A_1 < A_2$ the population $v(x, \tau)$ will wipe out at the end. However, the population $w(x, t)$ will remain alive for a long time life. The conclusion is that if the invasive population is weak, then the population will become extinct finally.

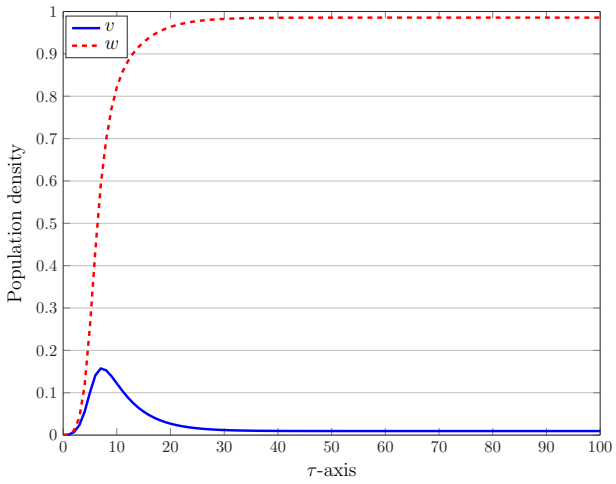

Figure 6. Graphing of population densities via Taylor-Touchard matrix algorithm in Example 1 with $Q = 5$, $A_1 = 0.8, A_2 = 1, B_1, B_2 = 1, C_1, C_2 = 1, D_1, D_2 = 1, \Delta\tau = 1$, at $x = 5$.

In the last experimental simulations for Example 1, let us investigate the competitive coexistence of two population species in the system. For this purpose, we set [17]

$$A_1 = 0.9, \quad A_2 = 1, \quad B_1, B_2 = 1, \quad C_1 = 0.8, C_2 = 1, \qquad D_1 = 0.3, D_2 = 1.$$

We run our Taylor-Touchard collocation matrix algorithm with a time step $\Delta\tau = 1$ as before. Using $Q = 5$ we get the next approximations evaluated at time $\tau = \Delta\tau$ as

$$v_{1,5}(x) = -3.9490{-}6\,x^5 + 0.000157353\,x^4 - 0.00245291\,x^3 + 0.0186658\,x^2 - 0.0692296\,x + 0.1,$$
$$w_{1,5}(x) = -2.7123{-}6\,x^5 + 0.000112368\,x^4 - 0.00184439\,x^3 + 0.0150341\,x^2 - 0.0611469\,x + 0.1.$$

The obtained approximations at the given final time $\tau = T$ are given by

$$v_{100,5}(x) = 0.000499975\,x^5 - 0.0157776\,x^4 + 0.177961\,x^3 - 0.872004\,x^2 + 1.69182\,x + 0.1,$$
$$w_{100,5}(x) = 0.0000344845\,x^5 - 0.00103192\,x^4 + 0.0109967\,x^3 - 0.0555938\,x^2 + 0.133343\,x + 0.1.$$

Besides the preceding polynomial solutions, we visualize the approximate solutions $v_{k,5}(x,\tau)$ and $w_{k,5}(x,\tau)$ for all $k = 1, 2, \ldots, 100$ in Figure 7 on the whole space-time domain $(x,\tau) \in [0,10] \times [0,100]$. The competition results of two populations for $(x,\tau) \in \{5\} \times [0,100]$ are shown in Figure 8.
From graphics presented in the former Figure 7 and Figure 8 one observes that both populations arrived at a coexistence state. In other words, the two competing species are equal in status, with neither complete victory nor loss in competition.

Example 2 *The second test example related to the Lotka-Volterra competition system* (2) *is devoted to the Neumann boundary conditions. That is, we take the following initial conditions*

$$f(x) = g(x) = 0.1\sin^2(2.4\,\pi\,x) + 0.28\sin^2(-0.05\,\pi\,x),$$

which is borrowed from [18]. The Neumann boundary conditions are set as follows:

$$v_0(\tau) = w_0(\tau) = f'(0), \quad v_L(\tau) = w_L(\tau) = f'(L).$$

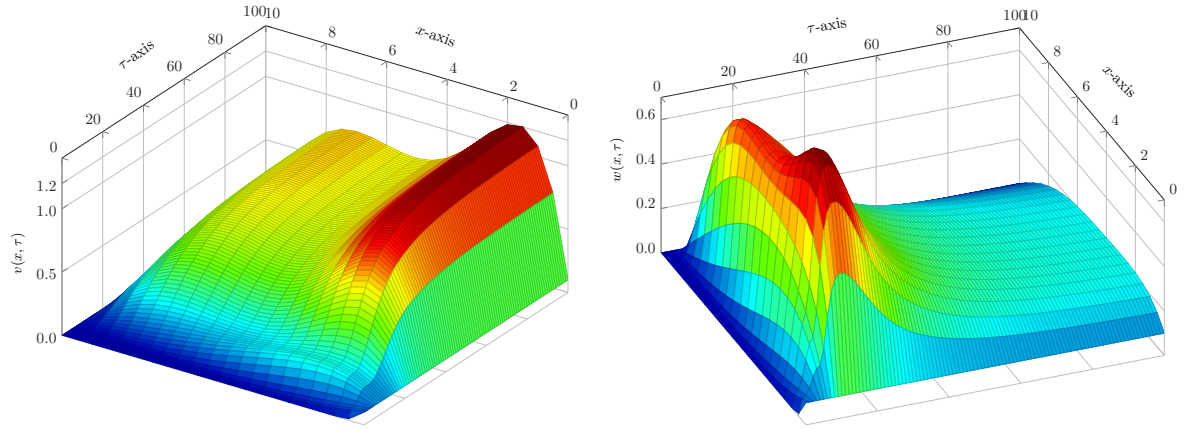

Figure 7. Visualization of approximate solutions $v(x,\tau)$ (left) and $w(x,\tau)$ (right) via Taylor-Touchard matrix algorithm in Example 1 with $Q=5$, $A_1=0.9, A_2=1, B_1, B_2=1, C_1=0.8, C_2=1, D_1=0.3, D_2=1, \Delta\tau=1$, for $(x,\tau)\in[0,10]\times[0,100]$

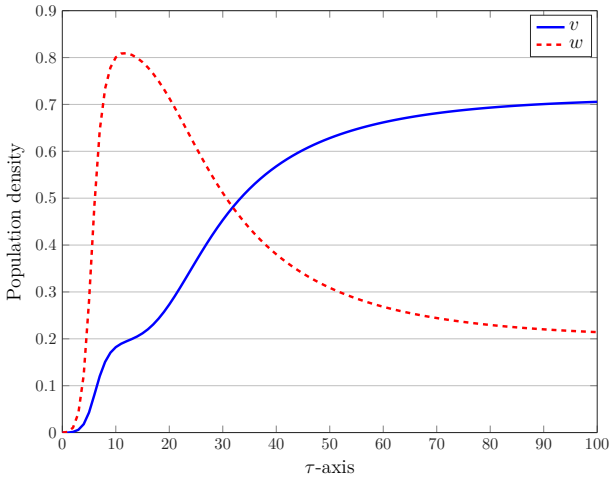

Figure 8. Visualization of population densities via Taylor-Touchard matrix algorithm in Example 1 with $Q=5$, $A_1=0.9, A_2=1, B_1, B_2=1, C_1=0.8, C_2=1, D_1=0.3, D_2=1, \Delta\tau=1$, at $x=5$

Below, we only use the coefficient parameters A_i, B_i, C_i, and D_i, for $i=1,2$ in the form

$$A_1=0.4, A_2=0.5,\quad D_1=D_2=0.001,\quad B_1=0.4, B_2=0.5,\quad C_1=0.5, C_2=0.8.$$

Using the aforementioned parameters and by running the Taylor-Touchard algorithm with $Q=5$ and $\Delta\tau=1$, we get the next approximate solutions computed at $\tau=\Delta\tau$ and for $0\le x\le 1$ as

$$\begin{aligned} v_{1,5}(x) &= 0.232195\,x^5-0.774398\,x^4+0.966988\,x^3-0.48004\,x^2-3.4{-}107\,x+0.145598,\\ w_{1,5}(x) &= 0.232362\,x^5-0.775521\,x^4+0.96977\,x^3-0.482383\,x^2-6.1{-}107\,x+0.153403. \end{aligned}$$

Similarly, at time level $\tau=T=100$, we get

$$\begin{aligned} v_{100,5}(x) &= -0.0137547\,x^5+0.0372937\,x^4-0.0340702\,x^3+0.0130377\,x^2\\ &\quad -1.7{-}108\,x+0.0183703,\\ w_{100,5}(x) &= -0.0139798\,x^5+0.0381177\,x^4-0.0346481\,x^3+0.0128192\,x^2+1.21895. \end{aligned}$$

In Figure 9, we present the above approximate solutions for $k = 1, 100$ together with other values $2 \leq k \leq 99$. While the left picture shows the population density v, the right plot depicts the approximate solution w on the whole domain $(x, \tau) \in [0, 1] \times [0, 100]$. At $x = 0.5$, we further plot the snapshots of approximation $v(x, \tau), w(x, \tau)$ over the long time domain $\tau \in [0, 100]$ as shown in Figure 10. If we look at Figure 9 and Figure 10, we can observe that the population v will eventually disappear and the population w will survive.

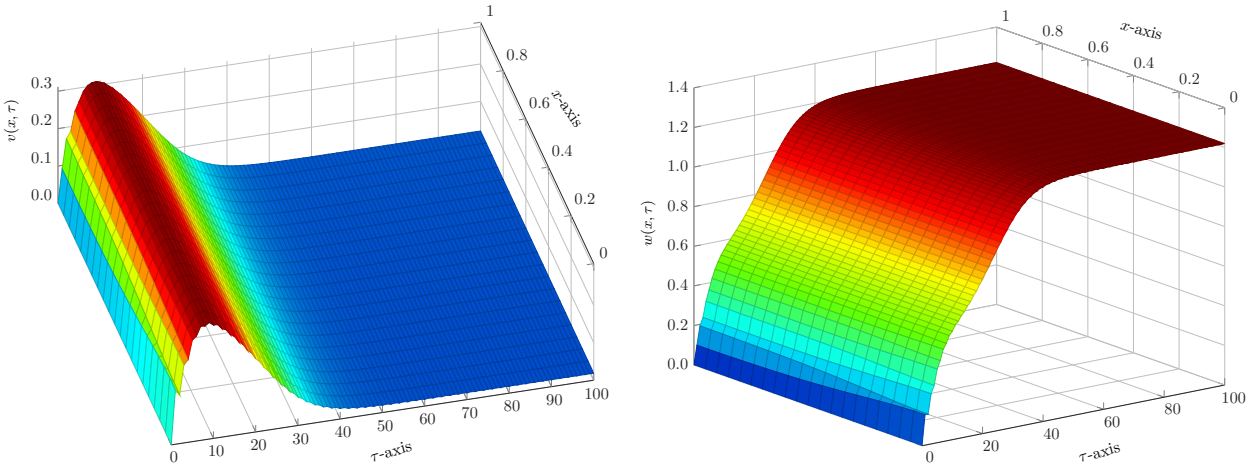

Figure 9. Visualization of approximate solutions $v(x, \tau)$ (left) and $w(x, \tau)$ (right) via Taylor-Touchard matrix algorithm in Example 2 with $Q = 5$, $A_1 = 0.4, A_2 = 0.5, B_1 = 0.5, B_2 = 0.4, C_1 = 0.5, C_2 = 0.8, D_1 = D_2 = 0.001$, $\Delta\tau = 1$, for $(x, \tau) \in [0, 1] \times [0, 100]$.

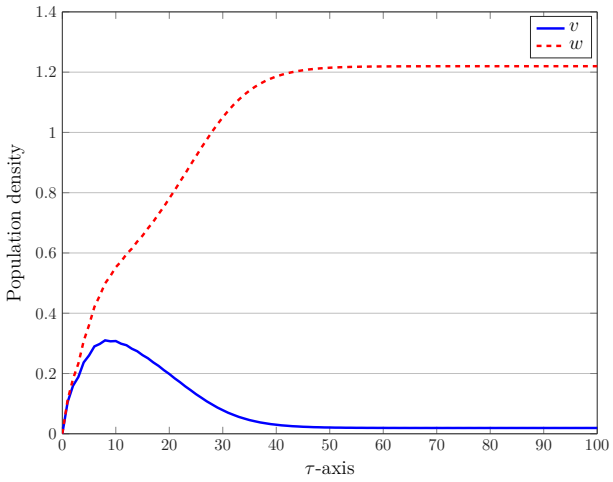

Figure 10. Graphing of population densities via Taylor-Touchard matrix algorithm in Example 2 with $Q = 5$, $A_1 = 0.4, A_2 = 0.5, B_1 = 0.5, B_2 = 0.4, C_1 = 0.5, C_2 = 0.8, D_1 = D_2 = 0.001, \Delta\tau = 1$, at $x = 5$.

In terms of achieved REFs, we fix $\Delta\tau = 0.01$ and consider two different values of $Q = 4, 8$ in the computations. The other parameters are given as above for the second test example. These REFs associated with the approximate solutions $v(x, \tau)$ and $w(x, \tau)$ are displayed in Figure 11. The time domain is $[0, 1]$ and the results are plotted at $x = 5$. The magnitude of REFs is decreased if one increases the number of basis functions Q.

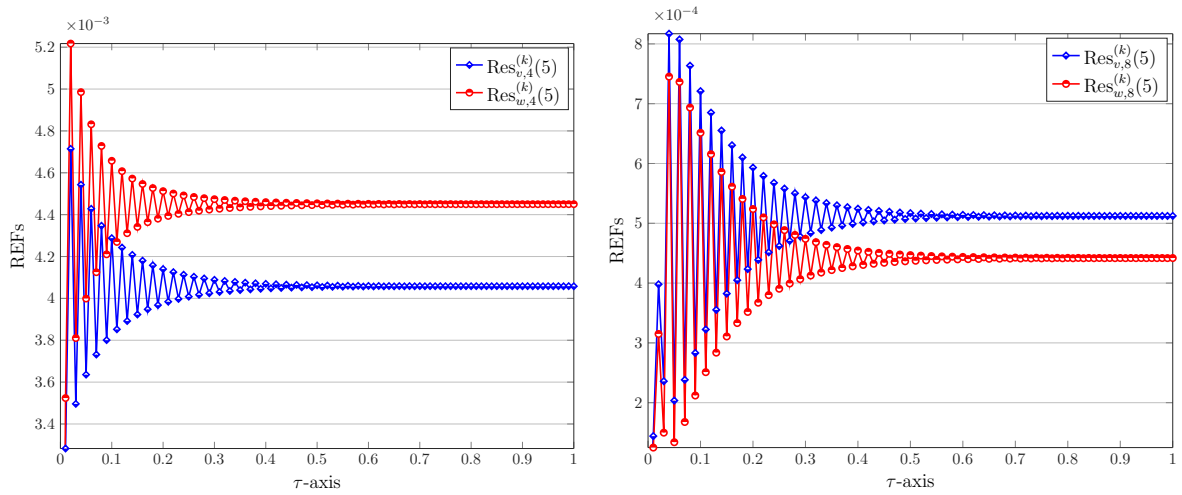

Figure 11. Visualization of REFs with $Q = 4$ (left) and $Q = 8$ (right) via Taylor-Touchard matrix algorithm in Example 2 with $A_1 = 0.4, A_2 = 0.5, B_1 = 0.5, B_2 = 0.4, C_1 = 0.5, C_2 = 0.8, D_1 = D_2 = 0.001, \Delta\tau = 0.01$, at $x = 5$

7 Conclusion

This study introduces a novel combined semi-discretized spectral matrix collocation algorithm for solving the Lotka-Volterra competition system with diffusion. The proposed algorithm utilizes the well-known Taylor series formula for the time-marching procedure and the Touchard family of polynomials for solving the resulting linear systems of ODEs using spectral matrix collocation. The convergence and error analysis of the proposed algorithm are discussed in detail. Additionally, a comprehensive qualitative analysis of the system is provided through stability analysis. Based on the performed stability analysis, equilibrium points for the system are obtained along with the conditions for a stable solution. Numerical simulations with diverse model parameters and boundary conditions are conducted to illustrate the applicability and effectiveness of the developed algorithm. The presented outcomes demonstrate that the proposed algorithm is accurate, efficient, and capable of providing stable solutions for the Lotka-Volterra competition system with diffusion. The residual error function technique is employed to further validate the accuracy and advantages of the proposed algorithm. Through the complete analysis, the accuracy of the proposed method increases with the number of used basis functions, validating the applicability of the method for solving similar complex problems.

This study makes significant contributions to the field of simulations of nonlinear PDEs and underscores the potential of the combined semi-discretized spectral matrix collocation algorithm for solving similar problems in diverse fields of science and engineering. The proposed algorithm serves as a powerful tool for modeling and simulating complex systems in areas such as ecology, biology, economics, and physics. Future research endeavors could extend the proposed algorithm to take into account other factors such as the extension of the current model to three or more species or incorporating the climate effect and investigate the effects of various parameters on the method's performance.

Declarations

Use of AI tools

The authors declare that they have not used Artificial Intelligence (AI) tools in the creation of this article.

Data availability statement

Data sharing is not applicable to this article as no datasets were generated or analyzed during the current study.

Ethical approval

Not applicable

Consent for publication

Not applicable

Conflicts of interest

The authors declare that they have no known competing financial interests or personal relationships that could have appeared to influence the work reported in this paper.

Funding

This research received no external funding.

Author's contributions

M.I.: Conceptualization, Methodology, Software, Investigation, Writing-original draft preparation, Writing-reviewing and editing. A.E.: Conceptualization, Methodology, Investigation, Writing-original draft preparation, Writing-reviewing and editing. W.A.: Conceptualization, Methodology, Investigation, Writing-original draft preparation, Writing-reviewing and editing. All authors have read and agreed to the published version of the manuscript.

Acknowledgements

The authors would like to convey many thanks to the Editor and Reviewers for their helpful comments and suggestions which further improved this study.

References

[1] Kumar, S., Kumar, A. and Odibat, Z.M. A nonlinear fractional model to describe the population dynamics of two interacting species. *Mathematical Methods in the Applied Sciences*, 40(11), 4134–4148, (2017). [CrossRef]

[2] Lotka, A.J. Contribution to the theory of periodic reactions. *The Journal of Physical Chemistry*, 14(3), 271-274, (2022). [CrossRef]

[3] Owolabi, K.M. Computational dynamics of predator-prey model with the power-law kernel. *Results in Physics*, 21, 103810, (2021). [CrossRef]

[4] Owolabi, K.M., Pindza, E. and Atangana, A. Analysis and pattern formation scenarios in the superdiffusive system of predation described with Caputo operator. *Chaos, Solitons & Fractals*, 152, 111468, (2021). [CrossRef]

[5] Pan, M.X., Wang, S.Y., Wu, X.L., Zhang, M.W. and Schiavo, A.L. Study on the growth driving model of the enterprise innovation community based on the Lotka–Volterra model: a case study of the Chinese Automobile Manufacturing Enterprise Community. *Mathematical Problems in Engineering*, 2022, 8743167, (2023). [CrossRef]

[6] Han, J. The Impact of epidemic infectious diseases on the ecological environment of three

species based on the Lotka–Volterra model. *World Scientific Research Journal*, 7(1), 340-345, (2021). [CrossRef]

[7] Ni, W., Shi, J. and Wang, M. Global stability and pattern formation in a nonlocal diffusive Lotka–Volterra competition model. *Journal of Differential Equations*, 264(11), 6891-6932, (2018). [CrossRef]

[8] Lin, G. and Ruan, S. Traveling wave solutions for delayed reaction–diffusion systems and applications to diffusive Lotka–Volterra competition models with distributed delays. *Journal of Dynamics and Differential Equations*, 26, 583-605, (2014). [CrossRef]

[9] Wijeratne, A.W., Yi, F. and Wei, J. Bifurcation analysis in the diffusive Lotka–Volterra system: an application to market economy. *Chaos, Solitons & Fractals*, 40(2), 902-911, (2009). [CrossRef]

[10] Cherniha, R. Construction and application of exact solutions of the diffusive Lotka–Volterra system: a review and new results. *Communications in Nonlinear Science and Numerical Simulation*, 113, 106579, (2022). [CrossRef]

[11] Zhang, S., Zhu, X. and Liu, X. A diffusive Lotka–Volterra model with Robin boundary condition and sign-changing growth rates in time-periodic environment. *Nonlinear Analysis: Real World Applications*, 72, 103856, (2023). [CrossRef]

[12] Ma, L., Gao, J., Li, D. and Lian, W. Dynamics of a delayed Lotka–Volterra competition model with directed dispersal. *Nonlinear Analysis: Real World Applications*, 71, 103830, (2023). [CrossRef]

[13] Barker, W. Existence of traveling waves of Lotka Volterra type models with delayed diffusion term and partial quasimonotonicity. *ArXiv Preprint, ArXiv:2303.11145*, (2023). [CrossRef]

[14] Guo, S. Global dynamics of a Lotka-Volterra competition-diffusion system with nonlinear boundary conditions. *Journal of Differential Equations*, 352, 308-353, (2023). [CrossRef]

[15] Kudryashov, N.A. and Zakharchenko, A.S. Analytical properties and exact solutions of the Lotka–Volterra competition system. *Applied Mathematics and Computation*, 254, 219-228, (2015). [CrossRef]

[16] Islam, M., Islam, B. and Islam, N. Exact solution of the prey-predator model with diffusion using an expansion method. *Applied Sciences*, 15, 85-93, (2013).

[17] Wang, J., Liu, Q. and Luo, Y. The numerical analysis of the long time asymptotic behavior for Lotka-Volterra competition model with diffusion. *Numerical Functional Analysis and Optimization*, 40(6), 685-705, (2019). [CrossRef]

[18] Sabawi, Y.A., Pirdawood, M.A. and Sadeeq, M.I. A compact fourth-order implicit-explicit Runge-Kutta type method for solving diffusive Lotka–Volterra system. In Proceedings, *Journal of Physics: Conference Series* (Vol. 1999, No. 1, p. 012103). *IOP Publishing*, (2021, April). [CrossRef]

[19] Izadi, M. Numerical approximation of Hunter-Saxton equation by an efficient accurate approach on long time domains. *UPB Scientific Bulletin Series A Applied Mathematics and Physics*, 83(1), 291-300, (2021).

[20] Izadi, M. and Yuzbasi, S. A hybrid approximation scheme for 1-D singularly perturbed parabolic convection-diffusion problems. *Mathematical Communications*, 27(1), 47-62, (2022).

[21] Izadi, M. and Roul, P. Spectral semi-discretization algorithm for a class of nonlinear parabolic PDEs with applications. *Applied Mathematics and Computation*, 429, 127226, (2022). [CrossRef]

[22] Izadi, M. and Zeidan, D. A convergent hybrid numerical scheme for a class of nonlinear

diffusion equations. *Computational and Applied Mathematics*, 41, 318, (2022). [CrossRef]

[23] Günerhan, H., Dutta, H., Dokuyucu, M.A. and Adel, W. Analysis of a fractional HIV model with Caputo and constant proportional Caputo operators. *Chaos, Solitons & Fractals*, 139, 110053, (2020). [CrossRef]

[24] El-Sayed, A.A., Baleanu, D. and Agarwal, P. A novel Jacobi operational matrix for numerical solution of multi-term variable-order fractional differential equations. *Journal of Taibah University for Science*, 14(1), 963-974, (2020). [CrossRef]

[25] Srivastava, H.M. and Izadi, M. Generalized shifted airfoil polynomials of the second kind to solve a class of singular electrohydrodynamic fluid model of fractional order. *Fractal and Fractional*, 7(1), 94, (2023). [CrossRef]

[26] Sabermahani, S., Ordokhani, Y. and Hassani, H. General Lagrange scaling functions: application in general model of variable order fractional partial differential equations. *Computational and Applied Mathematics*, 40, 269, (2021). [CrossRef]

[27] Abbasi, Z., Izadi, M. and Hosseini, M.M. A highly accurate matrix method for solving a class of strongly nonlinear BVP arising in modeling of human shape corneal. *Mathematical Methods in the Applied Sciences*, 46(2), 1511-1527, (2023). [CrossRef]

[28] Razavi, M., Hosseini, M.M. and Salemi, A. Error analysis and Kronecker implementation of Chebyshev spectral collocation method for solving linear PDEs. *Computational Methods for Differential Equations*, 10(4), 914–927, (2022). [CrossRef]

[29] Srivastava, H.M., Adel, W., Izadi, M. and El-Sayed, A.A. Solving some physics problems involving fractional-order differential equations with the Morgan-Voyce polynomials. *Fractal and Fractional*, 7(4), 301, (2023). [CrossRef]

[30] Izadi, M., Yüzbası, S. and Adel, W. Accurate and efficient matrix techniques for solving the fractional Lotka–Volterra population model. *Physica A: Statistical Mechanics and its Applications*, 600, 127558, (2022). [CrossRef]

[31] Mihoubi, M. and Maamra, M.S. Touchard polynomials, partial Bell polynomials and polynomials of binomial type. *Journal of Integer Sequences*, 14(3), (2011).

[32] Boyadzhiev, K.N. Exponential polynomials, Stirling numbers, and evaluation of some gamma integrals. *Abstract and Applied Analysis*, 2009, 168672, (2009). [CrossRef]

[33] Sabermahani, S. and Ordokhani, Y. A computational method to solve fractional-order Fokker-Planck equations based on Touchard polynomials. *Computational Mathematics and Computer Modeling with Applications (CMCMA)*, 1(2), 65-73, (2022). [CrossRef]

[34] Aldurayhim, A., Elsonbaty, A. and Elsadany, A.A. Dynamics of diffusive modified Previte-Hoffman food web model. *Mathematical Biosciences and Engineering*, 17(4), 4225-4256, (2020). [CrossRef]

[35] Ahmed, N., Elsonbaty, A., Raza, A., Rafiq, M. and Adel, W. Numerical simulation and stability analysis of a novel reaction–diffusion COVID-19 model. *Nonlinear Dynamics*, 106, 1293-1310, (2021). [CrossRef]

[36] Touchard, J. Sur les cycles des substitutions. *Acta Mathematica*, 70, 243-297, (1939). [CrossRef]

[37] Bell, E.T. Exponential polynomials. *Annals of Mathematics*, 35(2), 258-277, (1934). [CrossRef]

[38] Mansour, T. and Schork, M. The generalized Touchard polynomials revisited. *Applied Mathematics and Computation*, 219(19), 9978-9991, (2013). [CrossRef]

[39] Kim, T., Herscovici, O., Mansour, T. and Rim, S.H. Differential equations for p, q-Touchard

polynomials. *Open Mathematics*, 14(1), 908-912, (2016). [CrossRef]

[40] Comtet, L. The art of finite and infinite expansions. In Advanced Combinatorics (pp. xi-343). D. Reidel Publishing Co. Dordrecht, (1974).

[41] Harper, L.H. Stirling behavior is asymptotically normal. *The Annals of Mathematical Statistics*, 38(2), 410-414, (1967). [CrossRef]

[42] Isaacson, E. and Keller, H.B. *Analysis of Numerical Methods*. Courier Corporation: North Chelmsford, United States, (1994).

Mathematical Modelling and Numerical Simulation with Applications (MMNSA)
(https://dergipark.org.tr/en/pub/mmnsa)

How to cite this article: Izadi, M., El-Mesady, A. & Adel, W. (2024). A novel Touchard polynomial-based spectral matrix collocation method for solving the Lotka-Volterra competition system with diffusion. *Mathematical Modelling and Numerical Simulation with Applications*, 4(1), 37-65. https://doi.org/10.53391/mmnsa.1408997